Gene 819 (2022) 146246

Contents lists available at ScienceDirect

Gene

journal homepage: www.elsevier.com/locate/gene

Increase in ADAR1p110 activates the canonical Wnt signaling pathway associated with aggressive phenotype in triple negative breast cancer cells

Fernanda Morales [a,b], Paola Pérez [b,c], Julio C. Tapia [d], Lorena Lobos-González [e,h], José Manuel Herranz [g], Francisca Guevara [h], Pamela Rojas de Santiago [b,i], Esteban Palacios [j], Rodrigo Andaur [k,l], Eduardo A. Sagredo [a,b,m], Katherine Marcelain [a,k], Ricardo Armisén [f,*]

[a] Centro de Investigación y Tratamiento del Cáncer, Facultad de Medicina, Universidad de Chile, Independencia 1027, Santiago, Chile
[b] Center of Excellence in Precision Medicine, Pfizer Chile, Obispo Arturo Espinoza Campos 2526, Santiago, Chile
[c] NIDCR, National Institute of Health, 9000 Rockville Pike, Bldg 10, Room 1A01, Bethesda, MD, USA
[d] Programa de Biología Celular y Molecular, Instituto de Ciencias Biomédicas, Facultad de Medicina, Universidad de Chile, Independencia 1027, Santiago, Chile
[e] Centro De Medicina Regenerativa, Facultad de Medicina - Clínica Alemana, Universidad Del Desarrollo, Av. Las Condes 12496, Santiago, Chile
[f] Centro de Genética y Genómica, Instituto de Ciencias e Innovación en Medicina, Facultad de Medicina Clínica Alemana Universidad del Desarrollo, Av. Las Condes 12461, Edificio 3, oficina 205, CP 7590943, Santiago, Chile
[g] Departamento de Anatomía Patológica, Hospital Clínico Universidad de Chile, Santos Dumont 999, Santiago, Chile
[h] Fundación Ciencia & Vida – Andes Biotechnologies S.A., Av. Zanartu 1482, Santiago, Chile
[i] Departamento de Biología Celular y Molecular, Facultad de Ciencias Biológicas, Pontificia Universidad Católica de Chile, Avda. Libertador Bernardo ÓHiggins 340, Santiago, Chile
[j] Programa de Biología Celular y Molecular, Instituto de Ciencias Biomédicas, Facultad de Medicina, Universidad de Chile, Independencia 1027, Santiago, Chile
[k] Departamento de Oncología Básico Clínica, Facultad de Medicina, Universidad de Chile, Independencia 1027, Santiago, Chile
[l] Comisión Chilena de Energía Nuclear, Nueva Bilbao 12501, Las Condes, Santiago Chile
[m] Department of Molecular Biosciences, The Wenner-Gren Institute, Stockholm University, Svante Arrhenius väg 20C, 106 91 Stockholm, Sweden

ARTICLE INFO

Edited by: John Randolph Hawse

Keywords:
ADAR1
TNBC
Canonical Wnt pathway
Cell invasion
Breast cancer

ABSTRACT

Triple-negative breast cancer (TNBC) represents a challenge in the search for new therapeutic targets. TNBCs are aggressive and generate resistance to chemotherapy. Tumors of TNBC patients with poor prognosis present a high level of adenosine deaminase acting on RNA1 (ADAR1). We explore the connection of ADAR1 with the canonical Wnt signaling pathway and the effect of modulation of its expression in TNBC. Expression data from cell line sequencing (DepMap) and TCGA samples were downloaded and analyzed. We lentivirally generated an MDA-MB-231 breast cancer cell line that overexpress (OE) ADAR1p110 or an ADAR knockdown. Abundance of different proteins related to Wnt/β-catenin pathway and activity of nuclear β-catenin were analyzed by Western blot and luciferase TOP/FOP reporter assay, respectively. Cell invasion was analyzed by matrigel assay. In mice, we study the behavior of tumors generated from ADAR1p110 (OE) cells and tumor vascularization immunostaining were analyzed. ADAR1 connects to the canonical Wnt pathway in TNBC. ADAR1p110 overexpression decreased GSK-3β, while increasing active β-catenin. It also increased the activity of nuclear β-catenin and increased its target levels. ADAR1 knockdown has the opposite effect. MDA-MB-231 ADAR1 (OE) cells showed increased capacity of invasion. Subsequently, we observed that tumors derived from ADAR1p110 (OE) cells showed increased invasion towards the epithelium, and increased levels of Survivin and CD-31 expressed in vascular endothelial cells. These results indicate that ADAR1 overexpression alters the expression of some key

Abbreviations: TNBC, Triple-negative breast cancer; ADAR1, Adenosine Deaminases Acting on RNA1; LEF/TCF, lymphoid enhancer factor/T-cell factor; A, adenosine; I, inosine; RIP-seq, RNA immunoprecipitation; FBS, fetal bovine serum; DepMap, Cancer Dependency Map; TCGA, The Cancer Genome Atlas; GDC, Genomic Data Commons; FDR, False Discovery Rate; ATCC, American Type Cell Culture Collection; TPM, Transcript Per Million; MOI, multiplicity of infection; RT-qPCR, Reverse real-time quantitative PCR; WB, Western Blot; IFI, Indirect immunofluorescence; WT, wild-type; IHC, Immunohistochemistry; CD-31, Cluster of Differentiation-31; OE, overexpress; H/E, Hematoxylin/Eosin; SCTs, subcutaneous tumors; CML, Chronic Myeloid Leukemia; xFDR, False Discovery Ratex; FAK, Focal adhesion kinase; ESCC, Esophageal Squamous Cell Carcinoma; AZIN1, encoding antizyme inhibitor 1; LUAD, lung adenocarcinoma; HCC, human hepatocellular carcinoma.

* Corresponding author at: Centro de Genética y Genómica, Instituto de Ciencias e Innovación en Medicina, Facultad de Medicina Clínica Alemana Universidad del Desarrollo, Av. Las Condes 12461, Edificio 3, oficina 205, CP 7590943, Santiago, Chile.
E-mail address: rarmisen@udd.cl (R. Armisén).

https://doi.org/10.1016/j.gene.2022.146246
Received 20 July 2021; Received in revised form 13 December 2021; Accepted 18 January 2022
Available online 2 February 2022

components of the canonical Wnt pathway, favoring invasion and neovascularization, possibly through activation of the β-catenin, which suggests an unknown role of ADAR1p110 in aggressiveness of TNBC tumors.

1. Introduction

Breast cancer in females is the most diagnosed in the world, with an incidence of 24.5%, resulting in 15,5% of all deaths by cancers by 2018 (Sung et al., 2021). The triple negative breast cancer subtype lacks the expression of the Estrogen Receptor (RE^-), Progesterone Receptor (RP^-) and Human Epidermal growth factor Receptor-type 2 ($HER2^-$); represents 11.2% of all breast cancers (Dent et al., 2007), and has a poor prognosis and low survival after recurrence (Lin et al., 2008). Most deaths occur within 5 years after diagnosis (Dent et al., 2007), mainly due to its aggressive behavior (Irvin & Carey, 2008). TNBC presents elevated infiltration of tumor-associated macrophages (Yuan et al., 2014), invasion and metastasis to secondary organs (Neophytou et al., 2018), including ulcer formation (Sun et al., 2016). Also, TNBC tumors have been reported to have a higher density of blood microvessels than non-triple-negative tumors (Mohammed et al., 2011). Due to its heterogeneity and complexity, the players that regulate these processes in TNBC are still poorly known (Collignon et al., 2016).

The enzyme ADAR1 catalyzes the hydrolytic deamination of adenosine (A) producing inosine (I). There are two isoforms of ADAR1, one short - called p110 - expressed constitutively, and another long - called p150 - that is inducible by interferon (Patterson & Samuel, 1995). In estrogen-receptor-α–positive metastatic lobular breast cancer, ADAR1 is the only editing enzyme overexpressed (Shah et al., 2009) and basal-like PAM (Prediction Analysis of Microarray) 50 subtype patients with high levels of ADAR1 mRNA have a lower survival (Sagredo et al., 2018). Also, about 46% of TNBC have high expression of ADAR1 (Song et al., 2017), and the frequency of RNA editing in tumors is higher in breast cancer compared to healthy breast tissue (Fumagalli et al., 2015). Additionally, ADAR1–deficient TNBC cells lose the ability to generate tumors *in vivo*, demonstrating that TNBC cells require ADAR1 in tumorigenesis (Kung et al., 2021). On the other hand, in relation to the characteristics that promote tumor growth, the participation of ADAR1 in angiogenesis has been exposed in cervical cancer, where ADAR1 positive tumors show an increase in vascular invasion, and patients lower survival, and worse clinical prognosis, compared to ADAR1 negative tumors (Chen et al., 2017b). These investigations show the biological potential associated with changes in the expression of ADAR1. However, the exact role of ADAR1p110 in triple-negative breast cancer progression is yet undefined.

β-Catenin is a key component of the canonical Wnt signaling pathway. The activation of this pathway generates the translocation of β-catenin to the nucleus where it interacts with lymphoid enhancer factor/T-cell factor proteins (LEF/TCFs) and activates the transcription of genes like Cyclin D1, c–Myc and Matrix metallopeptidase-9 (MMP-9) (Shtutman et al., 1999; He et al., 1998) (Wu et al., 2007). In the inactive state of the pathway, Glycogen synthase kinase-3 beta (GSK-3β) phosphorylates β-catenin inducing its degradation in the proteasome (Saito-Diaz et al., 2013). In a mouse model, blocking the Wnt/β-catenin pathway inhibits the growth of tumors from triple negative breast cancer cells MDA–MB-231 (Wang et al., 2016), indicating that the deregulation of the Wnt/β–catenin pathway is involved in the progression of breast cancer (Mukherjee et al., 2012). Also, about 40% of primary breast cancers present high levels of cytoplasmic and nuclear β-catenin and correlates with poor prognosis and survival of patients (Incassati et al., 2010).

ADAR1 has been linked to the Wnt signaling pathway in Chronic Myeloid Leukemia (CML), where Wnt/β-catenin signaling pathway serves as a self-renewal pathway in progenitors of CML during progression to Blastic Crisis (BC). BC cells possess an in-frame splice deletion of the GSK-3β kinase domain due to missplicing. Due to the dysregulation of GSK-3β, the activation of β-catenin would be promoted, with an increase in the activation of β-catenin in BC CML, an increase in its translocation to the nucleus and high transcriptional activity (Abrahamsson et al., 2009). Also, it has been reported that high expression of ADAR1p150 promotes malignant reprogramming of myeloid progenitors (Jiang et al., 2013). In breast cancer, it is not clear in which cellular process the ADAR1p110 isoform might participate. In the RNA editing public Database of RNA Editing (DARNED) (Kiran & Baranov, 2010), we found that transcripts of β-catenin (CTNNB1) and GSK-3β (GSK3B) present adenosine (A) to inosine (I) editing (Bahn et al., 2012). Also, sequencing analysis of RNA immunoprecipitation (RIP–seq) in HeLa cells indicates that ADAR1p110 interacts with the transcripts of CTNNB1 and GSK3B (Galipon et al., 2017).

We hypothesized that ADAR1p110 promotes activation of the canonical Wnt pathway in TNBC, thereby inducing invasion and vascularization. Thus, we first studied the correlation of the expression of ADAR1 with key components of the canonical Wnt pathway in different TNBC cell lines, to later demonstrate the co-expression of ADAR1 with genes that encode proteins involved in signaling pathways that participate in the progression of TNBC. Next, we examine the effect of ADAR1p110 on the canonical Wnt pathway in MDA-MB-231 cells. We report that the overexpression of ADAR1p110 activates this signaling, inducing overexpression of some of its targets as Cyclin D1, c-Myc, MMP-9 and Survivin. Also, in subcutaneous tumors (SCTs) we show that ADAR1p110 is involved in the process of invasion and correlates with an increased neo-vascularization *in vivo* in MDA-MB-231 cells. In summary, we suggest ADAR1p110 as a new regulator of the canonical Wnt signaling pathway, and its role during invasion in TNBC.

2. Materials and methods

2.1. Correlation analysis between ADAR1 and components of the canonical Wnt pathway in breast cancer

The transcriptomic levels of ADAR1 (consider both isoforms) and components of the canonical Wnt pathway from 61 breast cancer cell lines were downloaded from the Cancer Dependency Map (DepMap) public database portal (https://depmap.org/portal/) [Expression Public 20Q4]. The breast cancer cell lines were filtered to obtain only 25 triple negative breast cancer cell lines. Correlation analysis between ADAR1 and the component of this transduction pathway was performed by Pearson correlation using Graph Pad Prism (Version 7.02v).

2.2. Pathway enrichment analysis of ADAR1 co-expressed genes in breast cancer

Gene expression and clinical data were obtained from The Cancer Genome Atlas (TCGA) Project (https://www.cancer.gov/tcga), breast cancer cohort (TCGA-BRCA) through the Genomic Data Commons (GDC) data portal (https://portal.gdc.cancer.gov/) (Grossman et al., 2016). Co-expression analysis of ADAR1 and protein-coding genes was performed using Pearson correlation method in R software v3.6.3 (R Core Team, 2020) in tumor samples and TNBC tumor samples. A Pearson coefficient $|\ r\ | \geq 0.2$ and a False Discovery Rate (FDR, Benjamini-Hochberg method) ≤ 0.05 was considered as cut-off criteria. Reactome database (https://reactome.org/) was used to perform the pathway enrichment analysis of ADAR1 co-expressed genes using Cytoscape software (https://cytoscape.org/) (Shannon et al., 2003) and ClueGO plugin v2.5.6 (Bindea et al., 2009).

2.3. Cell culture

The human breast cancer cell line MDA-MB-231 (ATCC, HTB-26) and epithelial breast cell line MCF-10A (ATCC, CRL-10317) was purchased from the American Type Cell Culture Collection (ATCC, Maryland, USA). MDA-MB-231 cells were cultured in Dulbecco's Modified Eagle's Medium/Ham's F-12 50/50 Mix (DMEM/F12, Corning) media supplemented with 10% heat-inactivated fetal bovine serum (FBS, Corning), 100 U/ml penicillin and 100 μg/mL streptomycin (Corning). In particular, the culture medium for MCF-10 cells was supplemented with 10% heat-inactivated horse serum (Corning), Recombinant Human Epidermal Growth Factor (EGF) 20 ng/mL (R&D Systems), Insulin 10 μg/mL (Sigma-Aldrich) and Hydrocortisone 100 μg/mL (Sigma-Aldrich). The cell cultures were maintained at 37 °C in a humidified atmosphere containing 5% CO_2. Cell lines were tested for contamination with mycoplasma using the EZ-PCR™ Mycoplasma Detection Kit (Biological Industries).

2.4. ADAR1 knockdown

MDA-MB-231 cell line was transduced using lentiviral vectors (GenTarget Inc) expressing a small hairpin RNA (shRNA) targeted against *ADAR1* transcript at a multiplicity of infection (MOI) of 10. The lentiviral vectors and their respective sequences correspond to: pLenti-U6-shRNA (TRCN0000336832) and pLenti-U6-shRNA (TRCN0000336886), called shRNA#1 and shRNA#2, respectively, using as control the pLenti-U6-shRNA vector (shControl) that lacks the shRNA insert. Puromycin 1.5 μg/ml (InvitroGen) for 48 h was used to select the stably transduced cells, to subsequently sorting the cells by monitoring the reporter signal Red Fluorescent Protein (RFP) that was encoded.

2.5. ADAR1p110 overexpression

The MDA-MB-231 cell line was transduced with the lentiviral vector ADAR1p110 (NM_001025107, GenTarget Inc) or with Mock control (Null-Control, GenTarget Inc) at a MOI of 5. Blasticidin 10 μg/ml (InvitroGen) for 48 h was used to select the stably transduced cells.

2.6. RNA isolation and Reverse real-time quantitative PCR (RT-qPCR)

Total RNA was extracted using Trizol® reagent (Life Technologies) and treated with deoxyribonuclease (DNase, TURBO DNA-free™ kit, Ambion). The RNA was quantified by UV absorbance with the BioTek™ Cytation 3™ (Thermo Fisher Scientific). One μg of total RNA was used to synthesize DNA complementary to RNA (cDNA) using the Affinity-Script™ RT-qPCR cDNA synthesis Kit (Agilent) using standard procedure. RT-qPCR was performed using Brilliant II SYBR® Green QPCR Master Mix (Agilent Technologies). Actin was used as housekeeping gene. At least three independent experiments were performed, and technical triplicates were measured, along with the no template control in an Eco Real-Time (Illumina) qPCR machine. The results are expressed as the fold of change relative to values obtained for Mock-transduced cells. The relative abundance of each mRNA was calculated using the $2^{-\Delta\Delta Ct}$ method. The programs and specific oligonucleotide primers (IDT DNA) used to amplify ADAR1, β-catenin, and MMP-9 are listed in Supplementary Table S1 and S2, respectively.

2.7. Protein extraction and Western blot

Total protein extracts were obtained from MDA-MB-231 in 80% confluent cultures in 100-mm^2 plates or tumor tissue. The cells were homogenized with radioimmunoprecipitation assay (RIPA) buffer (25 mM Tris-HCl, 150 mM NaCl, 1% NP-40, 1% sodium deoxycholate, 0.1% sodium dodecyl sulfate (SDS), pH 7.6 in the presence of a cocktail of protease (Calbiochem®) and phosphatase inhibitors (Roche) and then sonicated with Ultrasonic Homogenizer Systems (Sonic Ruptor 250, USA). Proteins are quantified using, Pierce ™ BCA Protein Assay kit (Thermo Scientific ™) and the absorbances were read at 562 nm in the BioTek™ Cytation 3™ equipment. The tumor tissues were disrupted in liquid nitrogen with a BioPulverizer (Biospec Products) and then protein extracted as described for the cell cultures. 25–45 μg total protein extracts were separated in gels of 8–12% SDS–PAGE depending on the protein to be evaluated. The resolved proteins were transferred to nitrocellulose membrane (Bio-Rad). The membranes were blocked with 5% bovine serum albumin (BSA) in buffer TTBS 1X (20 mM Tris, 137 mM de NaCl, 0,1% Tween-20, pH 7,6). Supplementary Table S3 and S4 list the antibodies and dilutions. The signal of the detection antibodies was observed using SuperSignal West Pico Chemiluminescent substrate (Thermo Fisher Scientific) and the images were revealed by exposing the membranes in the Chemiluminescence Imaging System (Clinx Science Instruments Co., Ltd.). The intensity of the signal detected was measured by densitometry using Image Studio Lite Western Blot Analysis software (LI-COR). The results were normalized by α-Tubulin or β–Actin protein levels.

2.8. Indirect Immunofluorescence (IFI) staining cultured cells

The cells were seed and grown in Chamber Slides System (Thermo Fisher Scientific) and were fixed in 3.7% formaldehyde solution (Sigma-Aldrich) for 15 min. After fixation the excess of fixative was rinsed using phosphate-buffered saline (PBS). 0.2% Triton X-100 PBS (Winkler) was used to permeabilized the cells and then blocked with 3% BSA in 0.2% Triton X-100 (Winkler) in PBS (Corning) for 45 min in a humid chamber at 4 °C. Primary antibodies were incubated overnight at 4 °C and secondary antibodies were incubated 45 min in a humid chamber at 4 °C in darkness. Supplementary Table S3 and S4 list the antibodies and dilutions. After the incubation and washing steps ProLong™ Gold Antifade Mountant with 4′,6-diamidino-2-phenylindole (DAPI, Thermo Fisher Scientific) was added to each condition and cover slips were mounted. The images were captured with the BX53 Fluorescence Microscope (Olympus, Japan). ImageJ software (NIH, Version 1.47) was used to analyze the images.

2.9. TCF/LEF TOP/FOP luciferase reporter assay

MDA-MB-231 cells were seeded in 6-well plates. 24 h post-seeding (approximately ~ 70% confluence) the MDA-MB-231 transduced cells were co-transfected with 1200 ng TOP-Flash or FOP–Flash with 200 ng control vector pRL-TK (Promega), using Lipofectamine 3000 (InvitroGen) according to the supplier instructions. 48 h post-transfection the luciferase activity was measured using the Dual Luciferase® Reporter Assay kit (Promega). The luciferase activity was measured using BioTek™ Cytation 3™ (Thermo Fisher Scientific). The activity of Top-Flash and Fop-Flash Firefly luciferase were normalized with Renilla luciferase activity, to finally obtain the TOP/FOP ratio. Each experiment was made in triplicate and technical triplicates were measured. As positive controls of the reporter assays two GSK-3β inhibitors were used independently at 24 h post-transfection, MDA–MB-231 cells were stimulated 24 h with 25 mM of lithium chloride (LiCl, Sigma-Aldrich) and 20 μM of SB–216763) (Fernández et al., 2014), using 25 mM of sodium chloride (NaCl, Merck) and 20 μM of dimethyl sulfoxide (DMSO, Sigma-Aldrich) as their respective controls.

2.10. Transwell migration assay

Cell migration assays were performed on Transwell chamber with insert of polycarbonate membrane of 8.0 μm (Corning) and 2 μg/mL Fibronectin (Sigma-Aldrich) was added to the bottom of the Transwell inserts and allowed to incubate overnight at 4 °C. Then $2x10^5$ homogenized cells were seeded on top of Transwell inserts in 200 μL of DMEM/F12 medium FBS free, and 500 μL of DMEM/F12 medium supplemented

with 10% SBF, used as a chemoattractant was added under the inserts in each well (Mendoza et al., 2013). After 24 h incubation at 37 °C in a humidified atmosphere and 5% CO_2, the culture medium was removed from the chambers and the non-migrated cells were removed with a cotton swab. The chambers were then immersed in 3.7% formaldehyde solution (Sigma-Aldrich) for fixed cells. Then, to stain the migrated cells, the chambers were immersed in a 0.1% Crystal Violet solution (Sigma-Aldrich) with methanol (Millipore). Ten images per condition were captured using BioTek™ Cytation 3™ (Thermo Fisher Scientific) and the number of cells per field was counted using the ImageJ software (NIH, Version 1.47).

2.11. Matrigel invasion assay

Transwell inserts of polycarbonate membrane of 8.0 μm pore covered with Matrigel (Corning) were incubated for two hours in DMEM/F12 (Corning) free medium fetal bovine serum (FBS) at 37 °C. $2x10^4$ cells MDA-MB-231 suspended in 500 μL of DMEM/F12 medium FBS free were seeded on the inserts. In the lower chamber 500 μL DMEM/F12 medium 10% FBS was used as a chemoattractant. The system was kept for 24 h at 37 °C in humidified atmosphere and 5% CO_2 (Mendoza et al., 2013). The cells that did not invade the matrigel were removed with a cotton swab. The filter inserts and embedded cell were fixed in 3.7% formaldehyde solution (Sigma-Aldrich) and permeabilized with 0.2% Triton X-100 in PBS (Winkler). The membranes were separated from the insert and placed on a slide. ProLong®-DAPI (Life-technologies) was added on top and coverslips mounted. Ten images per condition were captured with the BX53 Fluorescence Microscope (Olympus, Japan) and the number of cells nuclei per field was counted using the ImageJ software (NIH, Version 1.47).

2.12. Animals

Immunodeficient BALB/c NOD-SCID pathogen-free female mice of 12 weeks of age were from Jackson Laboratories (Bar Harbor, Maine, USA). Animals were randomly distributed in the experimental design and were kept in the bioterium of the Andes Biotechnologies. All the procedure and experimental conditions were approved by Facultad de Medicina at Universidad de Chile Animal Research Bioethics Committee, following the National Research Council of The National Academies (USA) guidelines for laboratory animals use and care.

2.13. Tumor growth assay

MDA-MB-231 wild-type (WT), MDA-MB-231 Mock (Mock) and MDA-MB-231 ADAR1p110 overexpress (ADAR1p110 (OE)) cells were seeded in flasks until they reached a maximum of 70% confluence. The cells were harvested with trypsin 1X (Corning) at 37 °C, trypsin was then inactivated with DMEM/F12, 10% FBS (ratio 2:1). The cells were centrifuged at 2000 r.p.m. for 5 min. The cell pellet was washed twice with sterile 0.9% NaCl and subsequently the cells were suspended in physiological saline solution sterile. The cells were counted using the Luna-FL™ Dual Fluorescence Cell Counter (Logos Biosystems), in duplicate. $2.5x10^6$ cells in 100 μL of 0.9% NaCl were injected subcutaneously in the back of the mice with regular protocol (Lobos-Gonzalez et al., 2014), in blind. Once the presence of the primary tumor was detected by palpation the volume of the tumor was periodically measured with caliper and recorded. Tumor Volume is measured as $= \text{width}^2 \times \text{length} \times \pi/6$.

2.14. Evaluation of cellular invasion in tumor

When observing the reddening of the skin, loss of hair and presence of scab in the subcutaneous tumors, mice were anesthetized with ketamine/xylazine (100:10 v/v) and the tumors were extracted by surgery. After surgery the animals were treated with palliative medication. The animals were maintained under close observation and managed in compliance with the established criteria for tumor models *in vivo* (Morton, 2000; "United Kingdom Co-ordinating Committee on Cancer Research (UKCCCR) Guidelines for the Welfare of Animals in Experimental Neoplasia (Second Edition)," 1998; Schuh, 2004). Consequently, animals that showed signs of tumor aggressiveness received euthanasia as needed before the day the study ended (day 58). At day 58 after inoculation, after euthanizing the animals, the subcutaneous tumors not removed previously were extracted. To evaluate the invasion of the epithelium in the animal SCTs, a histopathological analysis of Hematoxylin/Eosin (H/E) stains was performed in blind. Mouse image of the experimental diagram obtained from https://biorender.com/.

2.15. Immunohistochemistry (IHC)

Part of the tumor was fixed with 4% neutral paraformaldehyde and embedded in paraffin. Slices of 5 μm were deparaffinized in xylene and re-hydrated through battery of alcohols. For antigen recovery, Target Retrieval (DACO) was used for 20 min in a steamer. The slices were then treated with 3% H_2O_2 in PBS 1X for 10 min and blocked with 2% goat serum in 0,3% Triton X-100 PBS for 30 min. The primary antibodies were incubated overnight at 4 °C and were detected with DAB Substrate Kit (Abcam) Supplementary Table S3 and S4 lists the antibodies and dilutions. After detection the tissues were counter-stained with Contrast Blue. Finally, the tissue was dehydrated, and coverslip were mounted with Entellan® (Sigma-Aldrich). To analyze ADAR1 and Survivin, one section per tumor sample was used, and for Cluster of Differentiation-31 (CD-31), three sections were histopathologically analyzed (start, center, and end of the tissue sample). A negative control without primary antibody was performed as well. A histopathological analysis of CD-31 was performed and the blood vessels from the animal tissue surrounding the SCTs were discarded from the study. 5–15 images were captured for ADAR1 and Survivin; and 7–45 images were captured to analyze CD-31 in the endothelial cells that make up the blood vessels in primary tumors. The images were captured with the Leica Microsystem CMS GmbH (DM 1000 LED, Germany) microscope. The densitometry analysis was carried out using the Image Pro Plus 6.0v software to obtain the Density and the representative images were captured using digital slide scanner NanoZoomer XR (Hamamatsu Photonics, Japan).

2.16. Statistical analysis

Data analysis was performed using Graph Pad Prism (Version 7.02v). The data are presented as mean values of at least three independent experiments with S.D. or S.E.M. The data was tested with Kolmogorov-Smirnov to establish whether it has normal distribution or not. The non-parametric data was analyzed with the Mann-Whitney test, and the parametric Paired *t* test. The tumor volumes over time were analyzed by one-way ANOVA, and post-test analysis was performed using Tukey's multiple comparisons test. Differences were considered statistically significant when $p < 0.05$.

3. Results

3.1. Expression of ADAR1 relates to the canonical Wnt signaling pathway in TNBC

To investigate whether the expression of ADAR1 is related to the expression of key components of the canonical Wnt signaling pathway in breast cancer, the first step consisted in the analysis of the correlation between ADAR1 transcriptomic level and GSK3B, CTNNB1, BIRC5, CCND1, MYC, AKT1, AKT2, AKT3 transcriptomic level in 61 breast cancer cell lines (Supplementary Table 5). Transcript Per Million (TPM) expression analysis reveals that ADAR1 shows positive correlation with GSK3B, CTNNB1, BIRC5, MYC, AKT1, AKT2 (Fig. 1, green dots). Then, according to the negative expression of ER, PR and HER2, 25 TNBC cell

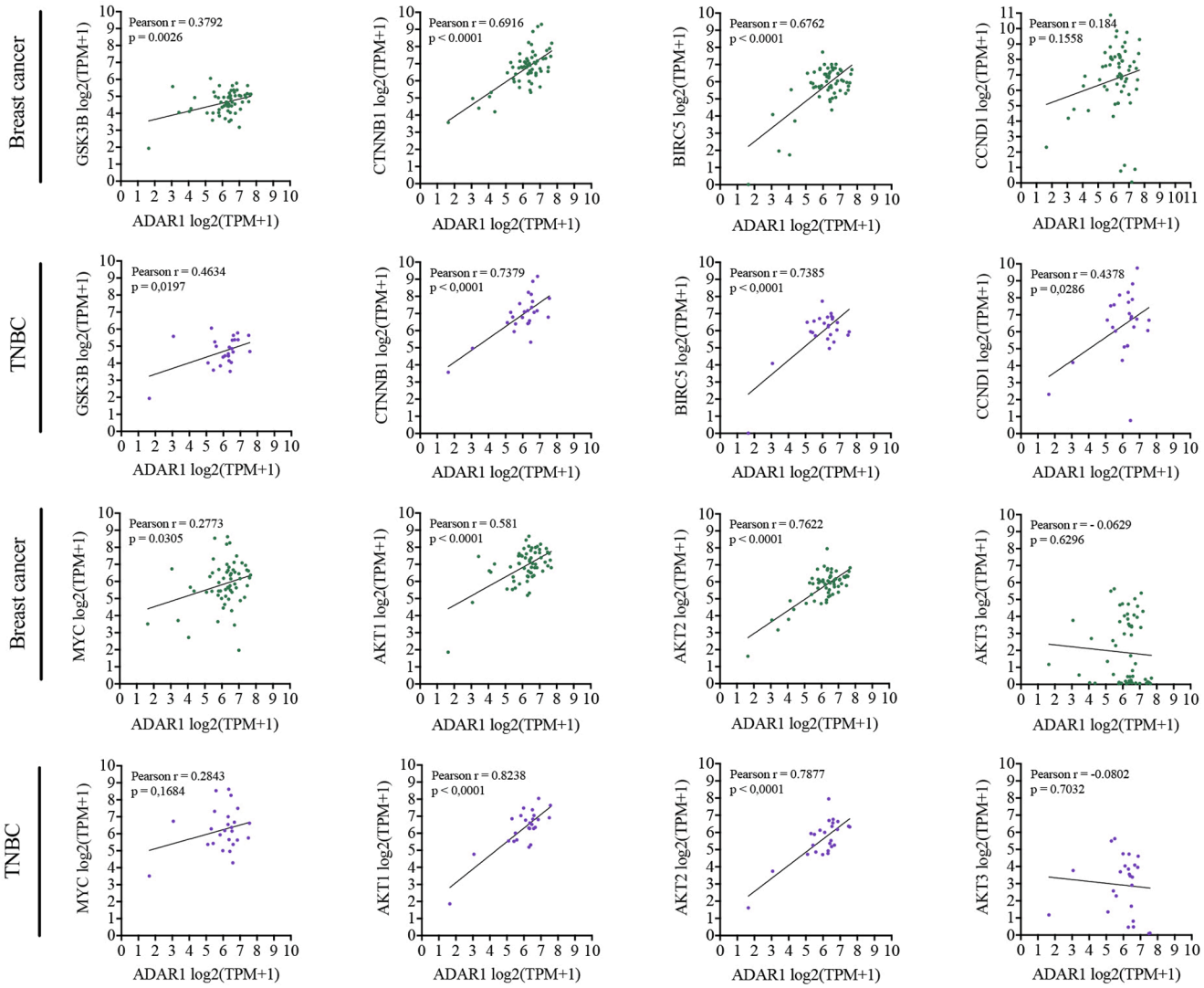

Fig. 1. Positive correlation between the expression of ADAR1 and the expression of components of the canonical Wnt signaling pathway in breast cancer cell lines. Correlation analysis between ADAR1 transcript level and GSK-3β (GSK3B), β-catenin (CTNNB1), Survivin (BIRC5), Cyclin D1 (CCND1), c-Myc (MYC), AKT1 (AKT1), AKT2 (AKT2), AKT3 (AKT3) transcript level in breast cancer cell lines (green dots, n = 61) and in TNBC cell lines (purple dots, n = 25). The graph shows the TPM expression levels for each gene. Data presented the Pearson correlation (r) and *p* value. **** $p < 0.0001$. (For interpretation of the references to colour in this figure legend, the reader is referred to the web version of this article.)

lines were evaluated (Supplementary Table 5). Consequently, we find that ADAR1 presents a positive correlation with GSK3B, CTNNB1, BIRC5, CCND1, AKT1 and AKT2 (Fig. 1, purple dots). MYC was not statistically significant. No correlation of ADAR1 with AKT3 was found in the evaluated cell lines (Fig. 1).

Then, we extended the study to analyze the protein-coding genes that are co-expressed with ADAR1 in tumor samples from public databases of breast cancer patients (TCGA-BRCA cohort), followed by a specific analysis for tumor samples from TNBC patients. The results showed that ADAR1 co–expressed protein-coding genes belonging to the signal transduction, organization of the extracellular matrix, signaling pathways related to β-catenin and with the vascularization process, through Vascular Endothelial Growth Factor (VEGF) signaling pathways (Fig. 2a and see Supplementary Table 6), among other gene ontologies (Supplementary Table 7). Interestingly, using clinical data from patients with TNBC, it was found that ADAR1 also is connected to signaling pathways related to the organization of the extracellular matrix, β-catenin, and VEGF. (Fig. 2b and see Supplementary Table 8), among other gene ontologies (Supplementary Table 9). Taken together, these results suggest that ADAR1 could be involved in the Wnt/β-catenin signaling pathway in TNBC.

3.2. *Overexpression of ADAR1p110 in MDA-MB-231 cells activates the canonical Wnt signaling pathway*

To assess the role of ADAR1p110 on the Wnt/β-catenin pathway in triple-negative breast cancer, we first turned to examine the protein level of ADAR1p110 in the non-tumor epithelial cell line, MCF-10, and in the MDA-MB-231 cell line, which is a widely accepted model for studying triple–negative subtype breast cancer (Chavez et al., 2011). In both cell lines quantifiable levels of the ADAR1p110 isoform were obtained, finding that the MDA-MB-231 metastatic breast cancer cell line has a lower content of ADAR1p110, with respect to MCF-10 cells (Fig. 3A). Next, ADAR1p110 was overexpressed by lentiviral transduction in a triple negative breast cancer cell line, generating two lines of MDA-MB-231: one transduced with a vector that overexpresses ADAR1p110 (ADAR1p110 (OE)) and another transduced with the empty vector (Mock). Quantitative PCR and Western blot analysis showed (Fig. 1B and 1C, respectively) that ADAR1p110 overexpression increased more than two-fold the basal level, both in transcript and

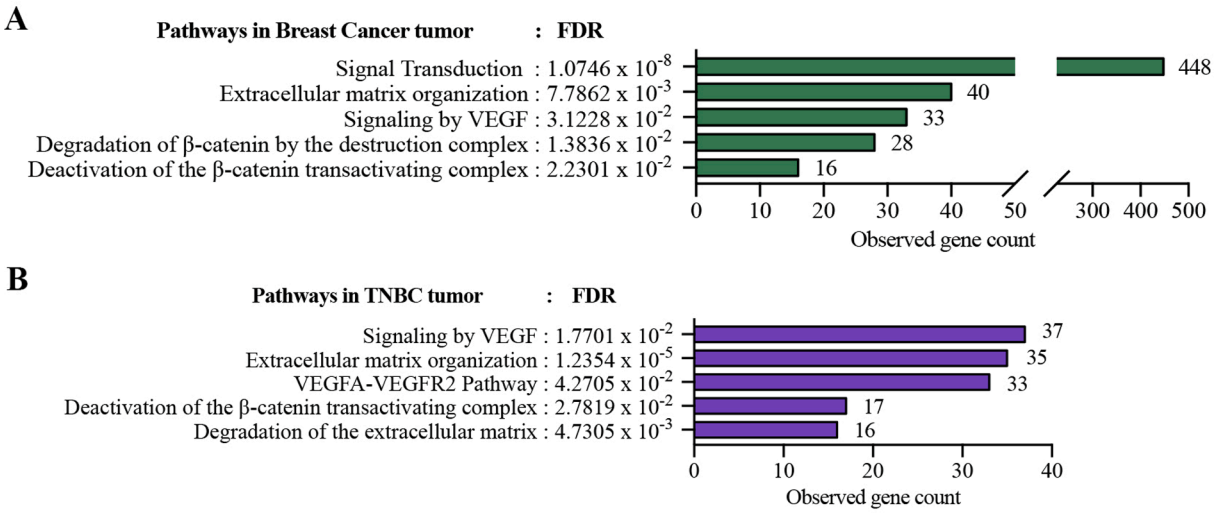

Fig. 2. ADAR1 expression is associated with components of the canonical Wnt signaling pathway in breast cancer. **a** Reactome pathway enrichment analysis for ADAR1 co-expressed protein-coding genes in tumor samples from TCGA-BRCA (n = 1097). **b** Reactome pathway enrichment analysis for ADAR1 co-expressed protein-coding genes in TNBC tumor samples from TCGA-BRCA cohort (n = 115). Significant pathways (FDR ≤ 0.05) related to β-catenin, VEGF, extracellular matrix and signal transduction pathways are depicted.

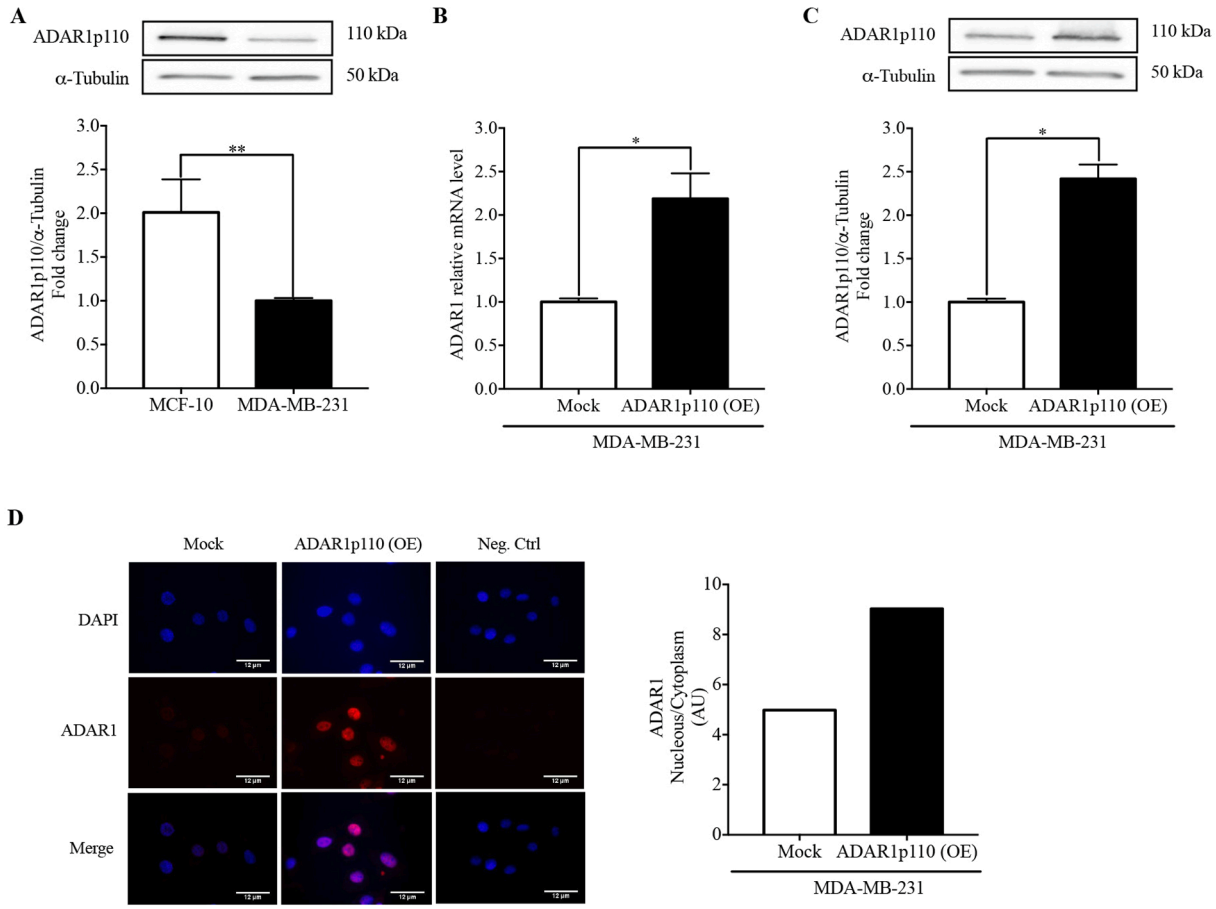

Fig. 3. Characterization of ADAR1p110 overexpression in MDA-MB-231 metastatic breast cancer cell line. **a** Protein levels of ADAR1p110 in MCF-10 and MDA-MB-231 were analyzed by Western blot. Representative blots are displayed. Data represent means of fold change relative to the MDA-MB-231 cells ± S.E.M; n = 5; ** $p < 0.01$. **b** After ADAR1p110 overexpression, transcript levels for ADAR1 analyzed by RT-qPCR. Results normalized to the expression of β-Actin (n = 4). Data correspond to mean of the fold change, relative to the Mock ± S.E.M, * $p < 0.05$. **c** After ADAR1p110 overexpression protein level of ADAR1p110 analyzed by Western blot. Representative blots are displayed, fold of change relative to the Mock condition. Data presented means ± S.E.M from n = 4; * $p < 0.05$ **d** Immunofluorescence of ADAR1 in MDA-MB-231 ADAR1p110 (OE) and MDA-MB-231 Mock cells. Nuclei stained with DAPI, images obtained at 60X. The graph shows the Nucleus/Cytoplasm ratio as arbitrary units (AU), data correspond from n = 1. Scale bar in all the pictures corresponds to 12 μm.

protein. Fluorescence microscopy analyses of total ADAR1 location suggested that ADAR1 increased its location in the nucleus as compared to the cytoplasm in OE cells (Fig. 3D). To study the activation of the canonical Wnt pathway, protein levels of critical components of this pathway, GSK-3β and β-catenin, were assessed. In cells ADAR1p110 (OE), levels of GSK-3β decreased (Fig. 4A) while β-catenin (Fig. 4B) and active β-catenin (i.e. not phosphorylated in Ser37/Thr41) increased (Fig. 4C) respect to Mock cells. No changes were detected in β-catenin mRNA levels (Fig. 4D). Accordingly, β-catenin protein levels are diminished in MDA-MB-231 ADAR1 knockdown cells (Fig. 5A and 5B).

Fluorescence microscopy was used to measure β-catenin location in ADAR1p110 (OE) cells. β–Catenin increased in the nucleus of ADAR1p110 (OE) compared to the Mock cells (Fig. 4F). Also, overexpression of ADAR1p110 induced ~ 24% activation of a TCF/LEF gene reporter (TOP/FOP luciferase reporter assay) compared to reporter activity in the Mock cells (Fig. 4G). This increase is close to the maximal Wnt/β-catenin signaling pathway activation achieved with the inhibitors of GSK–3β SB-216763 and LiCl, 39% and 41% respectively, used as positive controls (Supplementary Fig. S1).

To further confirm that the overexpression of ADAR1p110 activates the Wnt/β-catenin signaling pathway, protein levels of canonical key targets were evaluated. ADAR1p110 significantly induced an increase of the protein levels of Survivin, Cyclin D1 and c-Myc (Fig. 4H), compared to control cells. Accordingly, Survivin, Cyclin D1 and c-Myc protein

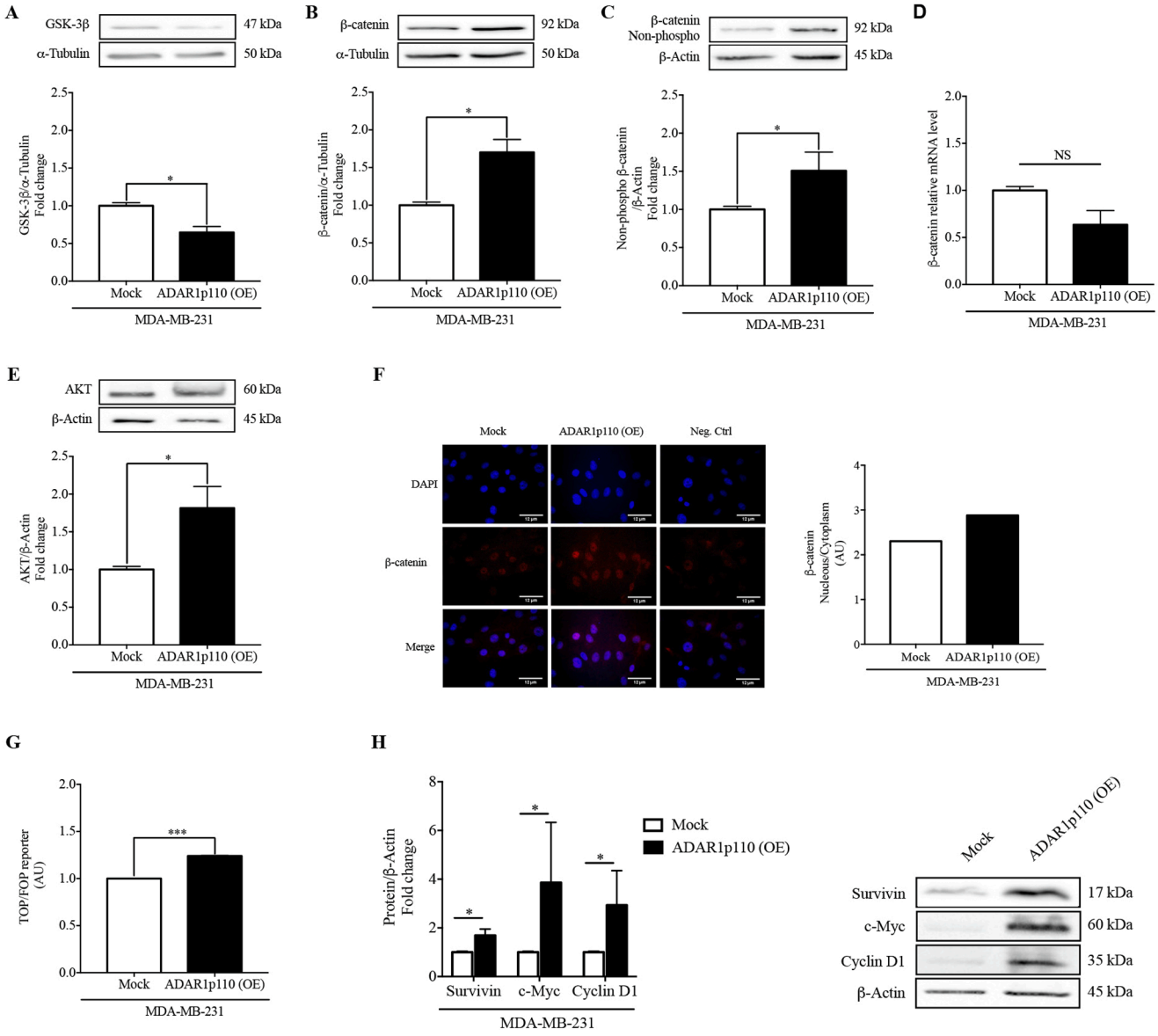

Fig. 4. Increased ADAR1p110 promotes the activation the canonical Wnt signaling pathway in MDA–MB-231 cell line. **a** Protein level of GSK-3β (n = 4); **b** β-catenin (n = 4) and **c** Non–phospho β–catenin (n = 4) analyzed by Western blot. Representative blots are displayed. The graph shows the densitometric analysis of the Western blots. Data correspond to mean of the fold change, relative to the Mock ± S.E.M; * $p < 0.05$. **d** RT-qPCR analysis of β-catenin transcript. Data was normalized to the expression of β-Actin (n = 4). Results correspond to mean of the fold change, relative to the Mock ± S.E.M. p greater than 0.05. **e** Immunofluorescence of analysis of β-catenin in MDA–MB–231 Mock cells and MDA-MB-231 ADAR1p110 (OE) cells. Nuclei were stained with DAPI. Images obtained at 60X. The graphs show the Nucleus/Cytoplasm ratio as arbitrary units (AU), data presented from n = 1. Scale bar in all the pictures corresponds to 12 μm. **f** Luciferase reporter activity in MDA-MB-231 Mock cells, and MDA-MB-231 ADAR1p110 (OE) cells using TOP/FOP reporter assay. Results are expressed with TOP/FOP (AU) and data correspond to mean of the fold change, relative to the Mock ± S.D, n = 3, *** $p < 0.01$. In the graph, S.D is a low value, for that reason the deviations are imperceptible. **g** The protein levels of Survivin, Cyclin D1 and c-Myc were analyzed by Western blot. Representative blots are displayed. Data represent means of fold change relative to the Mock condition ± S.E.M; n = 4; * $p < 0.05$.

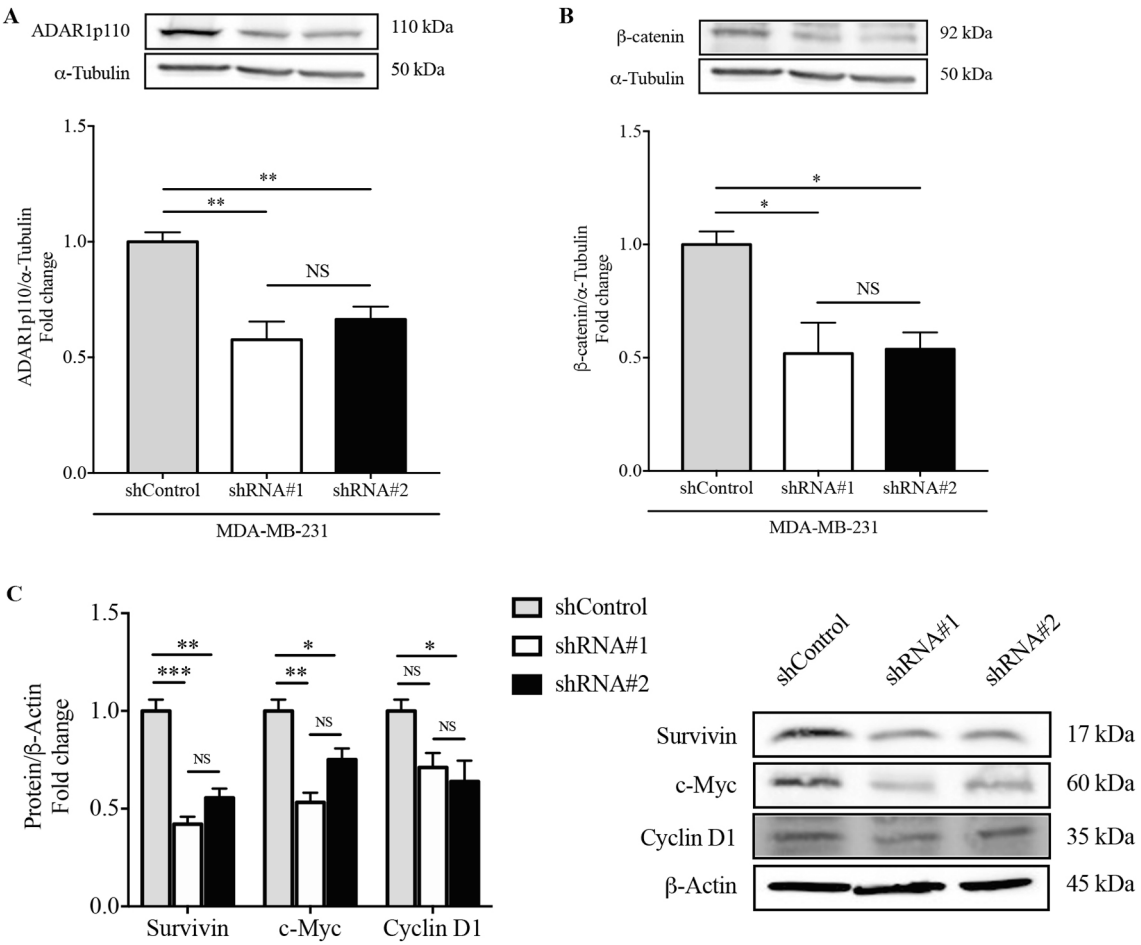

Fig. 5. Decreased ADAR1p110 induces the down regulation the canonical Wnt signaling pathway in MDA-MB-231 cell line. ADAR1 silencing effects on the (**a**) protein levels of ADAR1p110 (n = 4) and **(b)** β-catenin (n = 3) analyzed by Western blot. Representative blots are displayed, The graph shows the densitometric analysis of the Western blots. Data correspond to mean of the fold change, relative to the shControl condition ± S.E.M; * $p < 0.05$; ** $p < 0.01$. **c** The protein levels of Survivin, Cyclin D1 and c-Myc were analyzed by Western blot. Representative blots are displayed. Data represent means of fold change relative to the shControl condition ± S.E.M; n = 3; * $p < 0.05$; ** $p < 0.01$; *** $p < 0.001$; NS: no differences were found between the conditions.

levels are diminished in MDA–MB–231 total ADAR1 knockdown cells (Fig. 5C). Altogether, these results suggest that overexpression of ADAR1p110 promotes the stabilization and nuclear translocation of β-catenin to act as a positive modulator of the Wnt/β-catenin pathway in a TNBC cell line.

3.3. *ADAR1p110 induces cell invasion in vitro in MDA-MB-231 cells and in vivo in subcutaneous tumors*

To address the possible participation of ADAR1 in the remodeling of the extracellular matrix found in our previous *in silico* results, we decided to explore the effect of ADAR1p110 on cell invasion, performing matrigel assays with the MDA-MB-231 cells. The assay revealed that the ADAR1p110 (OE) cells are more invasive than the Mock cells (Fig. 6A). This increase in cell invasion was associated with an increase in mRNA levels of MMP-9 (Fig. 6B). In addition, a Transwell cell migration assay shows that ADAR1p110 (OE) cells display a larger migratory capacity than Mock cells (Fig. 6C).

To further examine the above finding *in vivo* we used a xenograft mice model. BALB/c NOD–SCID mice were injected subcutaneously with either MDA-MB-231 ADAR1p110 (OE), MDA-MB-231 Mock, or MDA-MB-231 parental cells. The tumor formation in each animal was examined by palpation daily. Tumors were palpable at 10th day post-inoculation, whose subsequent evaluation is outlined in Fig. 6D. On day 24 post-inoculation, a slight reddening of the skin and slight hair loss appeared in the primary tumor in 2 of 5 animals (40%) in MDA-MB-231 wild-type injected; in 3 of 5 animals (60%) in MDA-MB-231 Mock; and in 8 of 9 animals (88.9%) in MDA-MB-231 ADAR1p110 (OE) as indicated in Fig. 6E. Then, 100% of the SCTs in each condition were evaluated up to day 26 post-inoculation. At least one animal of each condition presented increased reddening of the skin, loss of hair and presence of scab or wound. Therefore, following the criteria of Morton (Morton, 2000), to ensure the welfare of the animals, primary tumors were resected. During the development of the study, the tumors were removed in 3 of 5 animals (60%) injected with MDA–MB–231 wild-type; in 4 of 5 animals (80%) injected with MDA-MB-231 Mock, and in 8 of 9 animals (88.9%) injected with ADAR1p110 (OE). No differences were found in the volumes of the tumors (Supplementary Fig. S2).

Therefore, the histopathological analysis of the tumors showed that none of the animals inoculated with wild-type cells presented skin lesion (0 of 5), and 1 of 5 animals (20%) inoculated with Mock cells presented skin lesion at a tumor volume of 1688 mm^3, in comparison to 5 of 9 animals (55.6%) inoculated with ADAR1p110 (OE) cells that presented visible skin lesion at a tumor volume of 870.8 ± 198.8 mm^3. The day on which the lesion was observed for each animal is also indicated in the graphs (Fig. 6E). In tissue sections stained with H/E, it was possible to appreciate the conservation of the skin in the tumor formed from wild-type cells and Mock cells. On the other hand, the massive invasion of the ADAR1p110 (OE) cells was observed from the inside of the tumor towards the skin of the animal, resulting in the focal loss of the epithelium.

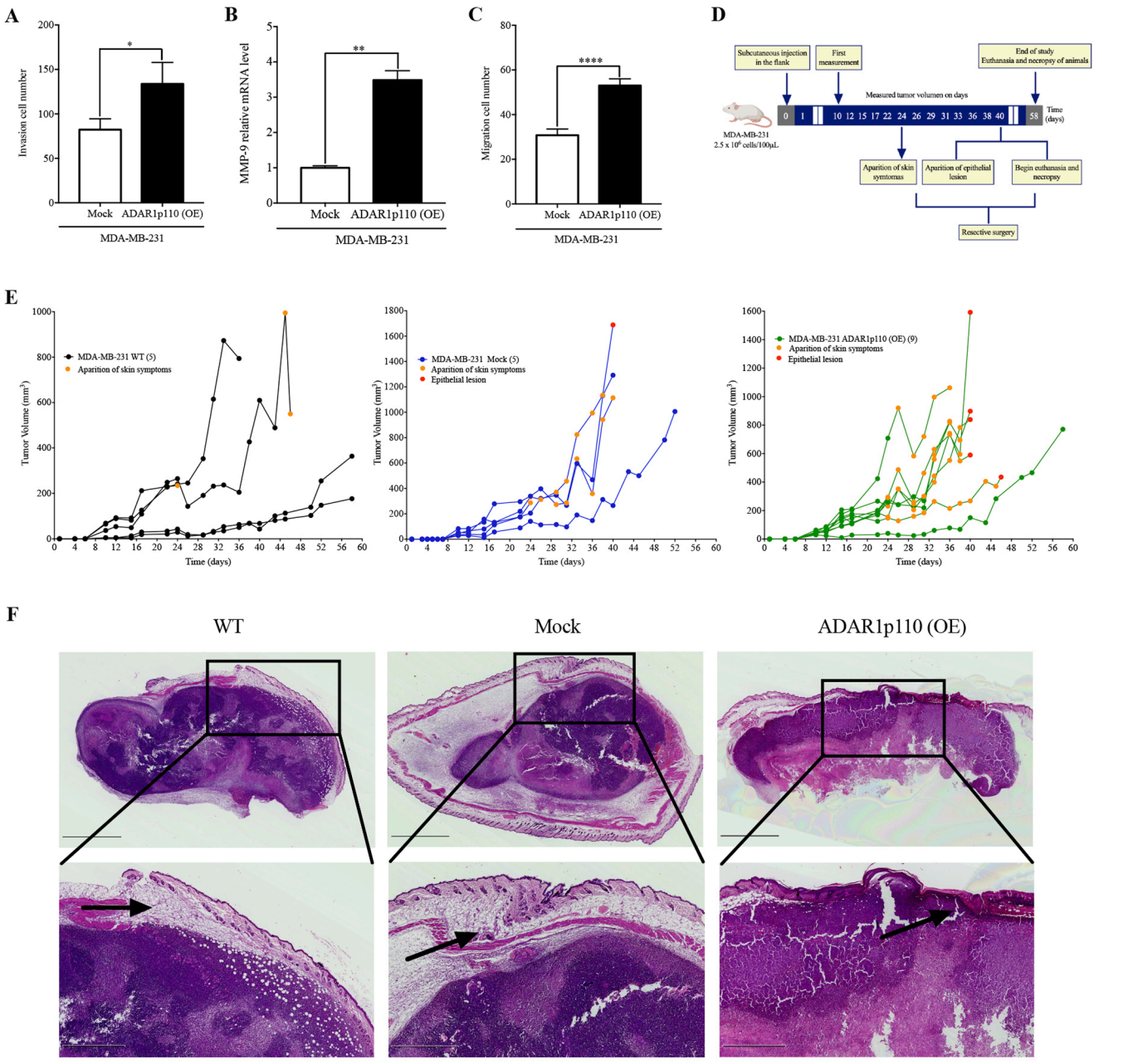

Fig. 6. ADAR1p110 overexpression in SCTs induces epithelial lesion *in vivo*. **a** Matrigel Invasion assay (n = 4), **b** MMP-9 transcript was analyzed by RT-qPCR (n = 3); **c** Transwell migration assay (n = 3). The results show the fold change, relative to the Mock, data are means ± S.E.M; * $p < 0.05$; ** $p < 0.01$; **** $p < 0.0001$. **d** Experimental design of *in vivo* tumorigenesis assay. BALB/c NOD–SCID female mice were inoculated subcutaneously in the flank with MDA-MB-231 cells. **e** Time course of the tumor volume in each animal inoculated with MDA-MB-231 wt cells (black) (n = 5 mice per group) and MDA-MB-231 Mock cells (blue) (n = 5 mice per group); and in green each animal inoculated with MDA-MB-231 ADAR1p110 (OE) cells (n = 9 mice per group). Orange points indicate appearance of skin symptoms (from day 24 after inoculation) and red points indicate epithelial lesion. For an animal of the Mock condition, an epithelial lesion was presented to a tumor volume of 1688 mm^3, and in the ADAR1p110 (OE) condition, 5 animal presented epithelial lesion to a tumor volume of 870,8 ± 198,8 mm^3 (Mean ± S.E.M). **f** Images of H/E staining of tumor sections observed in the different conditions from left to right. In purple, live tumor cells are observed, while necrotic tissue is present in the pink center of the tumor. Scale bar correspond to 2.5 mm. Selected area (black box) is magnified. Black arrows indicate the conserved epithelium where the epithelial is preserved of tumor formed from MDA-MB-231 wt and MDA-MB-231 Mock cells, and the epithelial invasion with loss of the epithelial structure of tumor formed from MDA-MB-231 ADAR1p110 (OE) cells are shown. Scale bar correspond to 1 mm. (For interpretation of the references to colour in this figure legend, the reader is referred to the web version of this article.)

In the wild-type condition, the only case of death of an animal with a final tumor volume of 794 mm^3 was presented, and in the histopathological analysis of the lung tissue, only one animal of this same condition developed pulmonary metastasis. Also, all the SCTs in this study presented inflammation and necrosis.

During the development of this study, carcinomatosis was observed in 2 of 9 (22.2%) animals inoculated with ADAR1p110 (OE) cells. The tumors reached a final volume at the time of surgery of 839 mm^3 and 898 mm^3, along with an invasion of tumor cells towards the thoracic space and peritoneum, respectively. All animals that presented aggressive tumor characteristics received euthanasia. In the wild-type condition, euthanasia was performed in 1 of 5 (20%) animals; in the Mock condition in 2 of 5 (40%) animals; and in the ADAR1p110 (OE) condition in 3 of 9 (33.3%) animals. Taken together, these results indicate that

overexpression of ADAR1p110 could confer an aggressive invasive capacity on a TNBC cell line.

3.4. ADAR1p110 is involved in the vascularization in vivo in subcutaneous tumors

Since our bioinformatics results connected ADAR1 with signaling pathways related to the process of vascularization in TNBC tumor, we analyzed *in vivo* the relationship of overexpression of ADAR1p110 in the Wnt/β-catenin pathway with the neovascularization process. We examined sections of tumors obtained in the xenograft model by immunohistochemistry. Tumors formed from MDA–MB–231 ADAR1p110 (OE) cells presented high levels of total ADAR1 compared to the tumors formed from MDA-MB-231 wt and MDA-MB-231 Mock cells (Fig. 7A). Also, protein levels of Survivin, a Wnt/β-catenin target related with apoptosis and neovascularization (Sanhueza et al., 2015), were higher than in controls, as well as they were observed both in the nucleus and in the cytoplasm (Fig. 7B).

During histological analysis and macroscopic observation, an apparent increase in the number of blood vessels in SCTs formed from MDA-MB-231 ADAR1p110 (OE) cells was found. Endothelial cells express CD-31 (Newman, 1999), a widely used as an angiogenesis marker (Sapino et al., 2001). When CD-31 was detected in subcutaneous tumors, positive labeling of CD-31 was found in endothelial cells of new blood vessels. The densitometry analysis of a large area of the tumor (3 tumor sections) showed that tumors formed by MDA-MB-231 ADAR1p110 (OE) cells contained a higher abundance of CD–31, compared to tumors formed by MDA-MB-231 wt and MDA-MB-231 Mock cells (Fig. 7C). Protein levels of ADAR1p110, Survivin and CD-31 were also determined in extracts of SCTs. The primary tumors formed from MDA-MB-231 ADAR1p110 (OE) presented high content of ADAR1p110, Survivin and CD-31, in comparison to tumors of control conditions (Fig. 7D). Therefore, our results implied that abundant ADAR1 could contribute to the ability to develop blood vessels in TNBC tumors.

4. Discussion

TNBC has an aggressive behavior characterized by distant recurrences compared to other subtypes of breast cancer (Dent et al., 2007). TNBC tumors possess high genomic heterogeneity which may explain the broad resistance to drugs exhibited by patients (Jhan & Andrechek, 2017). Nowadays there are important advances in new therapies for TNBC patients, including immunotherapy (Mediratta et al., 2020) and drugs for patients with a germline BRCA mutation (Robson et al., 2017). However, these monotherapies do not benefit all TNBC patients across the board. Implying that for both early and late stages of the disease, the primary treatment continues to be chemotherapy (Bianchini et al., 2016), thereby finding possible-signaling pathways involved in the aggressiveness that characterizes this subtype of cancer is crucial. In this sense, our studies and others have reported that aberrant expression of ADAR1 in breast cancer alters different biological processes in e.g., proliferation, apoptosis, variations in the expression of lncRNA (Fumagalli et al., 2015; Sagredo et al., 2020; de Santiago et al., 2021; Kung et al., 2021). In this way ADAR1 up-regulated is related to poor prognosis in breast cancer (Sagredo et al., 2018; Kung et al., 2021). A recent study highlights the requirement of ADAR1p150 in the survival of TNBC cell lines (Kung et al., 2021). However, the implication of ADAR1p110 in TNBC remains unclear.

Here, we aimed to study the effect of ADAR1p110 overexpression on the canonical Wnt pathway characterized by being active in TNBC and participating in multiple processes that favor the development of cancer (Bilir et al., 2013). To this purpose, analysis of public sequencing databases in cell lines followed by pathway enrichment analysis of ADAR1 co-express genes in TNBC identified that GSK-3β, β-catenin, Survivin, AKT1, AKT2 possess positive correlation with the expression of ADAR1 and that in turn, ADAR1 connects with signaling pathways related to β-catenin, respectively. Considering these findings, it is possible to infer that ADAR1 could be involved in modulation of the Wnt/β-catenin pathway in TNBC. Previous research showed that in CML ADAR1 relates to the deregulation of GSK-3β and with an increase in activated nuclear β-catenin (Abrahamsson et al., 2009) (Jiang et al., 2013). Although the activation of this pathway is canonically dependent on the Wnt ligand, our investigation showed that ADAR1p110 is a new intracellular modulator of it.

In our experiments, cells were lentiviral transduced as a batch and no single clones were derived for Mock or ADAR1p110 OE cells, trying to avoid clonal-selection derived phenotypes. We successfully in show that ADAR1p110 overexpression alters the expression levels of keys components of the canonical Wnt pathway along with their activation. MDA-MB-231 cells with abundant ADAR1 present a low protein level of GSK-3β and increase the basal activation of the canonical Wnt pathway in MDA–MB-231. On the other hand, GSK-3β can be inactivated by phosphorylation at Ser9 (Sutherland et al., 1993) by AKT (Cross et al., 1995), a kinase that is overexpressed in MDA-MB-231 ADAR1p110 (OE) cells, suggesting that the increase in ADAR1p110 could promote the inactivation of GSK-3β in an AKT-dependent manner. Meanwhile, analysis of the clinical data from patients with TNBC revealed that among the protein-coding genes that are co-expressed with ADAR1 in tumor samples are AKT1 and AKT2. Our results are consistent with previous reports. In this regard, investigations in leukemia cells indicate that ADAR1p110 interacts with the family of AKT kinases (AKT-1, AKT-2 and AKT-3), while unlike AKT-1 and AKT-2, AKT-3 is practically undetectable at the nuclear level. Nevertheless, in HEK293T cells ADAR1p110 is a substrate for AKT isoforms. Then, nuclear AKT inhibits the deaminase activity of ADAR1p110 by phosphorylation at Thr738, preferentially mediated by AKT-1 (Bavelloni et al., 2019). However, it should be added that ADAR1 also has functions independent of its RNA editing activity (Licht & Jantsch, 2017; Ota et al., 2013). Future studies could evaluate if ADAR1 induces the decrease of GSK-3β and an increase in the different isoforms of AKT in a dependent or independent way of its RNA editing activity in breast cancer cells. The other isoform of GSK-3 corresponds to GSK-3α, capable of attenuating co-transcriptional activity of β–catenin en Chinese hamster ovary (CHO) cells (Asuni et al., 2006) and like GSK-3β, GSK-3α has been considered an important study factor in leukemia (Banerji et al., 2012). Nevertheless, although GSK-3α and β are expressed ubiquitously (Woodgett, 1990) and functional redundant (Frame & Cohen, 2001), GSK-3α unlike GSK-3β has been studied to a lesser extent in breast cancer. Thus, in-depth experiments are needed to determine whether ADAR1p110 exerts any effect on GSK-3α in TNBC. The use of a mutated ADAR1 expression vector would be a suitable experimental tool to address alterations in the components that participate in the activation of the canonical Wnt pathway, as well as its negative feedback. Subsequently, we observed an increase of dephosphorylated β-catenin by Western blot and confirmed the activation of nuclear β-catenin by TOP/FOP assay. Our results further support the findings of previous studies connecting ADAR1 to the Wnt/β-catenin signaling pathway in cancer (Abrahamsson et al., 2009; Galipon et al., 2017). On the other hand, the overexpression of ADAR1p110 not affects the β-catenin mRNA levels. In this sense, TPM expression analysis reveals that ADAR1 shows positive correlation with CTNNB1 in breast cancer cell lines and as well, specifically in TNBC cell lines. Since the MDA-MB-231 cell line corresponds to the TNBC subtype Mesenchymal stem-like (168), it would be reasonable to evaluate the impact of the ADAR1p110 overexpression in other TNBC subtypes. Also, cells that overexpress ADAR1p110 show up–regulation of c-Myc and Cyclin D1, and cells knockdown for ADAR1 showed diminished levels of these proteins. Conversely, studies in HCT116 colon cancer cells described that an ADAR1 mutant defective in editing induces the increase in activity of a TCF4 reporter, while in epithelial intestinal cells the loss of ADAR1 induces transcription of c-Myc but not Cyclin D1 (Galipon et al., 2017). These findings suggest that the effect of ADAR1p110 on the Wnt/β–catenin pathway may be dependent on the type of cancer.

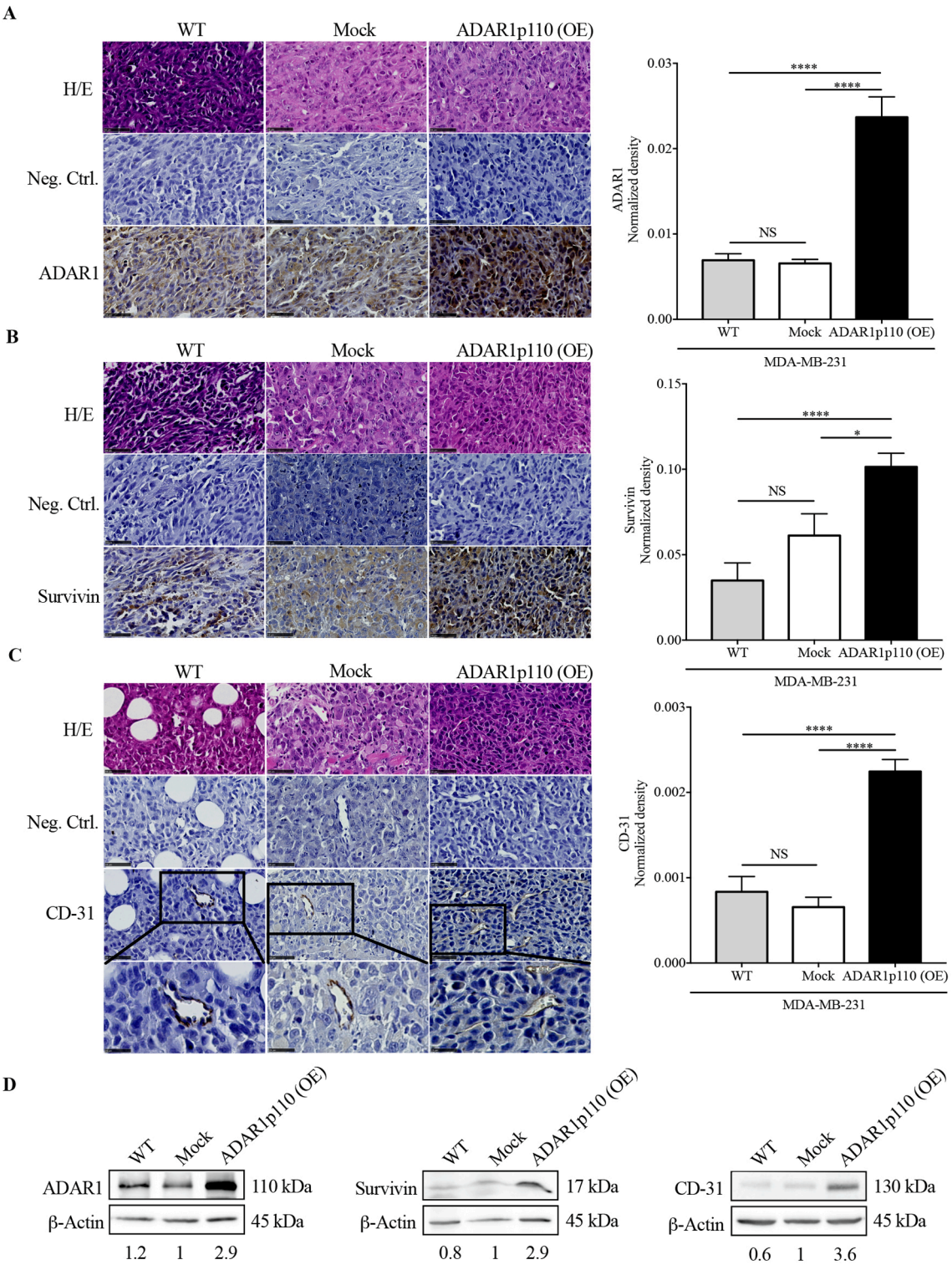

Fig. 7. Overexpression of ADAR1p110 correlates with neovascularización. *Ex vivo* immunohistochemistry analysis of ADAR1, Survivin and CD-31 in tumor sections from top to bottom are shown **(a, b** and **c)**. Representative staining images of tissue sections (40X) are shown throughout with H/E and negative control of SCT formed from MDA-MB-231 wild type cells (n = 4 mice per group), MDA-MB-231 Mock cells (n = 5 mice per group) and MDA-MB-231 ADAR1p110 (OE) cells (n = 9 mice per group). ADAR1 and Survivin are located both in nuclei and cytoplasm **(a** and **b**, respectively**)**. In **(c)** The marking in coffee corresponds to CD-31 present in endothelial cells that make up the micro-vessels. In the graphs the measurement by densitometry is expressed by Normalized Density and data represent means ± S.E. M; * $p < 0.05$, **** $p < 0.0001$. Scale bar in all the pictures correspond to 50 μm, blood vessels amplification are presented to a 25 μm scale bar. **d** In protein extracts from tumor samples the protein levels of ADAR1, Survivin and CD-31 were analyzed by Western blot. Densitometric analysis of representative blots are shown.

Although in TNBC the deregulation of the Wnt pathway and increased metastasis are already known (Dey et al., 2013), our work is the first report exploring the participation of ADAR1p110 in the activation of canonical Wnt pathway and its downstream effects on invasion. We found an increase in the invasive and migratory capacity in cells with high levels of ADAR1p110. Similarly, ADAR1p110 is the more expressed isoform and its silencing decreases invasion in human Esophageal Squamous Cell Carcinoma (ESCC) cells (Qin et al., 2014). Also, ADAR1 edits the transcript of Focal Adhesion Kinase (FAK) gene promoting invasion in Lung Adenocarcinoma (LUAD) cells (Amin et al., 2017). Moreover, human Hepatocellular Carcinoma (HCC) ADAR1p110 edits the transcript of Antizyme inhibitor 1 (AZIN1) gene, which induces a conformational change of AZIN1 protein, making it more stable. Cells that express edited AZIN1 present a higher invasive capacity, together with higher tumor growth (Chen et al., 2013). Additionally, MMP-9 is a transcriptional target dependent on the Wnt/β–catenin signaling pathway (Wu et al., 2007). In MDA-MB-231 cells, MMP-9 silencing reduces the invasive capacity characteristic of these cells by 90% (Mehner et al., 2014). Our data revealed that ADAR1 connects with gene ontology regarding extracellular matrix degradation and *in vitro* ADAR1 overexpression up-regulated the MMP-9 transcript. Thus, our analyzes add new evidence that supports the implication of ADAR1 in the process of cell invasion in cancer.

Thus, to expand our findings, we studied the impact of high levels of ADAR1p110 on tumor cells, which were subcutaneously inoculated in immunodeficient mice. The histopathological analysis of the tumors revealed massive areas of invasion by cancer cells that overexpressed ADAR1p110, which, unexpectedly, finally generated epidermal injury, confirming our *in vitro* findings. Interestingly, this injury is like that normally observed in stage IV of breast cancer (Güth et al., 2005) and TNBC (Sun et al., 2016). Also, ADAR1p110 induces the increase of active β-catenin. In murine excisional model, β–catenin participates in the cutaneous wound healing process, where abundant β-catenin is associated with larger wounds (Cheon et al., 2002; Cheon et al., 2006). In addition, epithelial lesions in tumors formed from cells that overexpressed ADAR1p110 were formed at lower tumor volumes compared to the SCT that presented epithelial lesions in the Mock condition. This would indicate that ADAR1p110 could be involved malignancy in TNBC cells through the activation of the canonical Wnt signaling pathway favoring invasive capacity in TNBC cells.

Survivin is an anti-apoptotic protein (Shin et al., 2001; Mita et al., 2008) overexpressed both *in vitro* and *in vivo* in our model of ADAR1p110. This is consistent with other studies in breast cancer showing induction of apoptosis after ADAR1 silencing (Fumagalli et al., 2015; Sagredo et al., 2020). In stressed cells, ADAR1p110 is phosphorylated at the nucleus and interacts with Exportin-5, thus allowing the export of Survivin towards the cytosol (Sakurai et al., 2017). Survivin also participates in angiogenesis by inducing VEGF in a β-catenin-dependent manner (Sanhueza et al., 2015; Fernández et al., 2014). In this study, our analyzes showed that ADAR1 also connects to VEGF-related signaling pathways in TNBC patients. VEGF induces the tyrosine phosphorylation of β–catenin, allowing the interaction with the adhesion protein CD-31, a recognized marker of angiogenesis (Sapino et al., 2001). CD-31 is expressed in endothelial cells of blood vessels, where it serves as a reservoir of β-catenin while maintaining its location at the plasma membrane (Ilan et al., 1999). In our study the positive CD–31 labeling in IHCs showed the presence of small blood vessels and a subsequent densitometric analysis showed an increase of CD-31 in tumors overexpressing ADAR1p110. These results are similar to observations in cervical carcinoma, where about 86% of ADAR1^{+} samples in patients have vascular invasion (Chen et al., 2017b). Thus, our data suggest that ADAR1p110 may promote tumor development by contributing to its blood supply.

A study conducted on ESCC cells that overexpress ADAR1p110 showed that changes in its expression are involved in cell transformation. Like our research, they studied the behavior of tumor volume in animals subcutaneously inoculated with cells that overexpress ADAR1p110, finding that ADAR1p110 induces the tumor growth rate, and the increase in tumor volume compared with the control condition (Qin et al., 2014). We analyze the tumor volume over time and throughout the study we had to perform surgery some animals, to remove tumors due to lesions in the epithelium, showing evidence of high aggressiveness. Since it was not possible to observe the growth of all primary developed tumors over the time of study, we cannot rule out that ADAR1p110 is required in tumorigenesis. Overall, results in this work and several others (Xu & Öhman, 2018) are increasingly showing that ADAR1 overexpression induces cancer growth in e.g., lung adenocarcinoma (Amin et al., 2017), cervical cancer (Chen et al., 2017a), hepatocellular carcinoma (Chen et al., 2013), esophageal cancer (Qin et al., 2014) and breast cancer (Nakano et al., 2017).

In our study the impact of ADAR1p110 on the Wnt/β-catenin pathway and the targets that this enzyme over-regulates was addressed. Given that many mRNAs are edited and more than 85% of pre–mRNAs are edited at intron sequences (Athanasiadis et al., 2004), we cannot rule out the role of other components of the canonical Wnt pathway. Future studies may contribute to define whether other pathways are affected by ADAR1p110 in TNBC.

5. Conclusions

In conclusion, our findings reveal that ADAR1p110 could be a new modulator of the canonical Wnt pathway and through this induces an invasive and migratory capacity in tumor cells as well as formation of new blood vessels, all-critical biological processes that allow the malignant progression of TNBC. We suggest that ADAR1p110 may function as an oncogene, which it may be evaluated as a new therapeutic approach for this cancer subtype.

Funding

This work was supported by Fondo Nacional de Desarrollo Científico y Tecnológico [FONDECYT regular grants 1151446, 1151435 and 1160889]; Comisión Nacional de Investigación Científica y Tecnológica [CONICYT Doctoral fellowships 21130317 and 21161206]. This work received institutional support from the Anillo en Ciencia y Tecnología [grant number ACT172101 and ACT210079], Fondo de Fomento al Desarrollo Científico y Tecnológico [FONDEF grant number IT16I10051], Fondo de Financiamiento de Centros de Investigación en Áreas Prioritarias [FONDAP grant 15130011] and Corporación de Fomento de la Producción [CORFO grant number 13CEE2-21602] initiatives. Funding sources were not involved in study design; the collection, analysis, and interpretation of data; in the writing of the report; and in the decision to submit the article for publication.

Ethics approval

All the procedure and experimental conditions were approved by Facultad de Medicina at Universidad de Chile Animal Research Bioethics Committee (protocol CBA 0763 FMUCH), following the National Research Council of The National Academies (USA) guidelines for laboratory animals use and care. The "Comité de Bioética de Investigación en Animales de Experimentación" at Fundación Ciencia & Vida provided further advice and experiments supervision. The Ethics committee of Facultad de Medicina, Universidad de Chile, approved the study (protocol 015-2015), to follow the Helsinki Declaration, the International Ethical Guidelines for Health-related Research Involving Humans CIOMS 2002 and the ICH 1996 Guidelines for Good Clinical Practice.

CRediT authorship contribution statement

Fernanda Morales: Conceptualization, Investigation, Validation, Methodology, Data curation, Formal analysis, Visualization, Funding

acquisition, Writing – original draft, Writing – review & editing. **Paola Pérez:** Data curation, Formal analysis, Visualization, Writing – original draft, Writing – review & editing. **Julio C. Tapia:** Conceptualization, Methodology, Investigation, Funding acquisition, Writing – review & editing. **Lorena Lobos-González:** Methodology, Investigation, Visualization, Data curation, Formal analysis, Writing – review & editing. **José Manuel Herranz:** Methodology, Investigation, Data curation, Formal analysis. **Francisca Guevara:** Methodology, Investigation, Data curation, Formal analysis. **Pamela Rojas de Santiago:** Methodology, Investigation, Data curation, Formal analysis. **Esteban Palacios:** Data curation, Formal analysis. **Rodrigo Andaur:** Methodology, Investigation, Data curation, Formal analysis. **Eduardo A. Sagredo:** Data curation, Formal analysis. **Katherine Marcelain:** Writing – review & editing, Funding acquisition. **Ricardo Armisén:** Conceptualization, Supervision, Investigation, Methodology, Validation, Visualization, Data curation, Formal analysis, Writing – original draft, Writing – review & editing, Funding acquisition.

Declaration of Competing Interest

The authors declare that they have no known competing financial interests or personal relationships that could have appeared to influence the work reported in this paper.

Acknowledgments

The results shown here are in part based upon data generated by the TCGA Research Network: https://www.cancer.gov/tcga. The authors thank M.Sc Jessica Toro, M.Sc Daniela Diez and Verónica Silva for their assistance in performing experiments, as well as PhD. Alfredo Sagredo for lentiviral transduction in MDA-MB-231 cell line.

Availability of data and material

The data used and analyzed in this study are available from the corresponding author on reasonable request.

Appendix A. Supplementary data

Supplementary data to this article can be found online at https://doi.org/10.1016/j.gene.2022.146246.

References

Abrahamsson, A.E., Geron, I., Gotlib, J., Dao, K.-H.-T., Barroga, C.F., Newton, I.G., Jamieson, C.H.M., 2009. Glycogen synthase kinase 3 missplicing contributes to leukemia stem cell generation. Proc. Natl. Acad. Sci. 106 (10), 3925–3929. https://doi.org/10.1073/pnas.0900189106.

Amin, E.M., Liu, Y., Deng, S.u., Tan, K.S., Chudgar, N., Mayo, M.W., Sanchez-Vega, F., Adusumilli, P.S., Schultz, N., Jones, D.R., 2017. The RNA-editing enzyme ADAR promotes lung adenocarcinoma migration and invasion by stabilizingFAK. Sci. Signaling 10 (497). https://doi.org/10.1126/scisignal.aah3941.

Asuni, A.A., Hooper, C., Reynolds, C.H., Lovestone, S., Anderton, B.H., Killick, R., 2006. GSK3alpha exhibits beta-catenin and tau directed kinase activities that are modulated by Wnt. Eur. J. Neurosci. 24 (12), 3387–3392. https://doi.org/10.1111/j.1460-9568.2006.05243.x.

Athanasiadis, A., Rich, A., Maas, S., Marv Wickens, 2004. Widespread A-to-I RNA editing of Alu-containing mRNAs in the human transcriptome. PLoS Biol. 2 (12), e391. https://doi.org/10.1371/journal.pbio.0020391.

Bahn, J.H., Lee, J.-H., Li, G., Greer, C., Peng, G., Xiao, X., 2012. Accurate identification of A-to-I RNA editing in human by transcriptome sequencing. Genome Res. 22 (1), 142–150. https://doi.org/10.1101/gr.124107.111.

Banerji, V., Frumm, S.M., Ross, K.N., Li, L.S., Schinzel, A.C., Hahn, C.K., Kakoza, R.M., Chow, K.T., Ross, L., Alexe, G., Tolliday, N., Inguilizian, H., Galinsky, I., Stone, R.M., DeAngelo, D.J., Roti, G., Aster, J.C., Hahn, W.C., Kung, A.L., Stegmaier, K., 2012. The intersection of genetic and chemical genomic screens identifies GSK-3α as a target in human acute myeloid leukemia. J. Clin. Invest. 122 (3), 935–947.

Bavelloni, A., Focaccia, E., Piazzi, M., Raffini, M., Cesarini, V., Tomaselli, S., Orsini, A., Ratti, S., Faenza, I., Cocco, L., Gallo, A., Blalock, W.L., 2019. AKT-dependent phosphorylation of the adenosine deaminases ADAR-1 and -2 inhibits deaminase activity. FASEB J. 33 (8), 9044–9061. https://doi.org/10.1096/fj.201800490RR.

Bianchini, G., Balko, J.M., Mayer, I.A., Sanders, M.E., Gianni, L., 2016. Triple-negative breast cancer: challenges and opportunities of a heterogeneous disease. Nat. Rev. Clin. Oncol. 13 (11), 674–690. https://doi.org/10.1038/nrclinonc.2016.66.

Bilir, B., Kucuk, O., Moreno, C.S., 2013. Wnt signaling blockage inhibits cell proliferation and migration, and induces apoptosis in triple-negative breast cancer cells. J. Transl. Med. 11 (1), 280. https://doi.org/10.1186/1479-5876-11-280.

Bindea, G., Mlecnik, B., Hackl, H., Charoentong, P., Tosolini, M., Kirilovsky, A., . . . Galon, J., 2009. ClueGO: a Cytoscape plug-in to decipher functionally grouped gene ontology and pathway annotation networks. Bioinformatics, 25, 8, 1091–1093. https://doi.org/10.1093/bioinformatics/btp101.

Chavez, K.J., Garimella, S.V., Lipkowitz, S., Eng-Wong, J., Zujewski, J.A., 2011. Triple negative breast cancer cell lines: One tool in the search for better treatment of triple negative breast cancer. Breast Disease 32 (1-2), 35–48.

Chen, L., Li, Y., Lin, C.H., Chan, T.H.M., Chow, R.K.K., Song, Y., . . . Guan, X.-Y., 2013. Recoding RNA editing of AZIN1 predisposes to hepatocellular carcinoma. Nat. Med., 19, 2, 209–216. https://doi.org/10.1038/nm.3043.

Chen, W., He, W., Cai, H., Hu, B., Zheng, C., Ke, X., Xie, L.i., Zheng, Z., Wu, X., Wang, H., 2017a. A-to-I RNA editing of BLCAP lost the inhibition to STAT3 activation in cervical cancer. Oncotarget 8 (24), 39417–39429.

Chen, Y., Wang, H., Lin, W., Shuai, P., 2017b. ADAR1 overexpression is associated with cervical cancer progression and angiogenesis. Diagn Pathol 12 (1), 12. https://doi.org/10.1186/s13000-017-0600-0.

Cheon, S.S., Cheah, A.Y.L., Turley, S., Nadesan, P., Poon, R., Clevers, H., Alman, B.A., 2002. Catenin stabilization dysregulates mesenchymal cell proliferation, motility, and invasiveness and causes aggressive fibromatosis and hyperplastic cutaneous wounds. Proc. Natl. Acad. Sci. 99 (10), 6973–6978. https://doi.org/10.1073/pnas.102657399.

Cheon, S.S., Wei, Q., Gurung, A., Youn, A., Bright, T., Poon, R., Whetstone, H., Guha, A., Alman, B.A., 2006. Beta-catenin regulates wound size and mediates the effect of TGF-beta in cutaneous healing. FASEB J 20 (6), 692–701. https://doi.org/10.1096/fj.05-4759com.

Collignon, J., Lousberg, L., Schroeder, H., Jerusalem, G., 2016. Triple-negative breast cancer: treatment challenges and solutions. Breast Cancer (Dove Med Press) 8, 93–107. https://doi.org/10.2147/BCTT.S69488.

Cross, D.A., Alessi, D.R., Cohen, P., Andjelkovich, M., Hemmings, B.A., 1995. Inhibition of glycogen synthase kinase-3 by insulin mediated by protein kinase B. Nature 378 (6559), 785–789. https://doi.org/10.1038/378785a0.

de Santiago, P.R., Blanco, A., Morales, F., Marcelain, K., Harismendy, O., Sjöberg Herrera, M., Armisén, R., 2021. Immune-related lncRNA LINC00944 responds to variations in ADAR1 levels and it is associated with breast cancer prognosis. Life Sci. 268, 118956. https://doi.org/10.1016/j.lfs.2020.118956.

Dent, R., Trudeau, M., Pritchard, K.I., Hanna, W.M., Kahn, H.K., Sawka, C.A., Lickley, L.A., Rawlinson, E., Sun, P., Narod, S.A., 2007. Triple-Negative Breast Cancer: Clinical Features and Patterns of Recurrence. Clin. Cancer Res. 13 (15), 4429–4434.

Dey, N., Barwick, B.G., Moreno, C.S., Ordanic-Kodani, M., Chen, Z., Oprea-Ilies, G., Tang, W., Catzavelos, C., Kerstann, K.F., Sledge, G.W., Abramovitz, M., Bouzyk, M., De, P., Leyland-Jones, B.R., 2013. Wnt signaling in triple negative breast cancer is associated with metastasis. BMC Cancer 13 (1). https://doi.org/10.1186/1471-2407-13-537.

Fernández, J.G., Rodríguez, D.A., Valenzuela, M., Calderon, C., Urzúa, U., Munroe, D., Rosas, C., Lemus, D., Díaz, N., Wright, M.C., Leyton, L., Tapia, J.C., Quest, A.FG., 2014. Survivin expression promotes VEGF-induced tumor angiogenesis via PI3K/Akt enhanced β-catenin/Tcf-Lef dependent transcription. Mol. Cancer 13 (1). https://doi.org/10.1186/1476-4598-13-209.

Frame, S., Cohen, P., 2001. GSK3 takes centre stage more than 20 years after its discovery. Biochem. J. 359 (Pt 1), 1–16. https://doi.org/10.1042/0264-6021:3590001.

Fumagalli, D., Gacquer, D., Rothé, F., Lefort, A., Libert, F., Brown, D., Kheddoumi, N., Shlien, A., Konopka, T., Salgado, R., Larsimont, D., Polyak, K., Willard-Gallo, K., Desmedt, C., Piccart, M., Abramowicz, M., Campbell, P., Sotiriou, C., Detours, V., 2015. Principles Governing A-to-I RNA Editing in the Breast Cancer Transcriptome. Cell Reports 13 (2), 277–289. https://doi.org/10.1016/j.celrep.2015.09.032.

Galipon, J., Ishii, R., Suzuki, Y., Tomita, M., Ui-Tei, K., 2017. Differential Binding of Three Major Human ADAR Isoforms to Coding and Long Non-Coding Transcripts. Genes 8 (2), 68. https://doi.org/10.3390/genes8020068.

Grossman, R.L., Heath, A.P., Ferretti, V., Varmus, H.E., Lowy, D.R., Kibbe, W.A., Staudt, L.M., 2016. Toward a Shared Vision for Cancer Genomic Data. N. Engl. J. Med. 375 (12), 1109–1112. https://doi.org/10.1056/nejmp1607591.

Güth, U., Singer, G., Schötzau, A., Langer, I., Dieterich, H., Rochlitz, C., Herberich, L., Holzgreve, W., Wight, E., 2005. Scope and significance of non-uniform classification practices in breast cancer with non-inflammatory skin involvement: a clinicopathologic study and an international survey. Ann. Oncol. 16 (10), 1618–1623. https://doi.org/10.1093/annonc/mdi319.

He, T.-C., Sparks, A.B., Rago, C., Hermeking, H., Zawel, L., da Costa, L.T., Morin, P.J., Vogelstein, B., Kinzler, K.W., 1998. Identification of c-MYC as a target of the APC pathway. Science 281 (5382), 1509–1512.

Ilan, N., Mahooti, S., Rimm, D.L., Madri, J.A., 1999. PECAM-1 (CD31) functions as a reservoir for and a modulator of tyrosine-phosphorylated beta-catenin. J. Cell Sci. 112 (Pt 18), 3005–3014.

Incassati, A., Chandramouli, A., Eelkema, R., Cowin, P., 2010. Key signaling nodes in mammary gland development and cancer: β-catenin. Breast Cancer Res. 12 (6), 213. https://doi.org/10.1186/bcr2723.

Irvin, W.J., Carey, L.A., 2008. What is triple-negative breast cancer? Eur. J. Cancer 44 (18), 2799–2805. https://doi.org/10.1016/j.ejca.2008.09.034.

Jhan, J.-R., Andrechek, E.R., 2017. Triple-negative breast cancer and the potential for targeted therapy. Pharmacogenomics 18 (17), 1595–1609. https://doi.org/10.2217/pgs-2017-0117.

Jiang, Q., Crews, L.A., Barrett, C.L., Chun, H.-J., Court, A.C., Isquith, J.M., Zipeto, M.A., Goff, D.J., Minden, M., Sadarangani, A., Rusert, J.M., Dao, K.-H.- T., Morris, S.R., Goldstein, L.S.B., Marra, M.A., Frazer, K.A., Jamieson, C.H.M., 2013. ADAR1 promotes malignant progenitor reprogramming in chronic myeloid leukemia. Proc. Natl. Acad. Sci. 110 (3), 1041–1046. https://doi.org/10.1073/pnas.1213021110.

Kiran, A., Baranov, P.V., 2010. DARNED: a DAtabase of RNa EDiting in humans. Bioinformatics 26 (14), 1772–1776. https://doi.org/10.1093/bioinformatics/btq285.

Kung, C.-P., Cottrell, K.A., Ryu, S., Bramel, E.R., Kladney, R.D., Bao, E.A., Freeman, E.C., Sabloak, T., Maggi, L., Weber, J.D., 2021. Evaluating the therapeutic potential of ADAR1 inhibition for triple-negative breast cancer. Oncogene 40 (1), 189–202. https://doi.org/10.1038/s41388-020-01515-5.

Licht, K., Jantsch, M.F., 2017. The Other Face of an Editor: ADAR1 Functions in Editing-Independent Ways. BioEssays 39 (11), 1700129. https://doi.org/10.1002/bies.v39.1110.1002/bies.201700129.

Lin, N.U., Claus, E., Sohl, J., Razzak, A.R., Arnaout, A., Winer, E.P., 2008. Sites of distant recurrence and clinical outcomes in patients with metastatic triple-negative breast cancer. Cancer 113 (10), 2638–2645. https://doi.org/10.1002/cncr.23930.

Lobos-Gonzalez, L., Aguilar-Guzmán, L., Fernandez, J.G., Muñoz, N., Hossain, M., Bieneck, S., Silva, V., Burzio, V., Sviderskaya, E.V., Bennett, D.C., Leyton, L., Quest, A.F.G., 2014. Caveolin-1 is a risk factor for postsurgery metastasis in preclinical melanoma models. Melanoma Res. 24 (2), 108–119.

Mediratta, K., El-Sahli, S., D'Costa, V., Wang, L., 2020. Current Progresses and Challenges of Immunotherapy in Triple-Negative Breast Cancer. Cancers 12 (12), 3529. https://doi.org/10.3390/cancers12123529.

Mehner, C., Hockla, A., Miller, E., Ran, S., Radisky, D.C., Radisky, E.S., 2014. Tumor cell-produced matrix metalloproteinase 9 (MMP-9) drives malignant progression and metastasis of basal-like triple negative breast cancer. Oncotarget 5 (9), 2736–2749. https://doi.org/10.18632/oncotarget.1932.

Mendoza, P., Ortiz, R., Díaz, J., Quest, A.F., Leyton, L., Stupack, D., Torres, V.A., 2013. Rab5 activation promotes focal adhesion disassembly, migration and invasiveness in tumor cells. J. Cell Sci. 126 (Pt 17), 3835–3847. https://doi.org/10.1242/jcs.119727.

Mita, A.C., Mita, M.M., Nawrocki, S.T., Giles, F.J., 2008. Survivin: Key Regulator of Mitosis and Apoptosis and Novel Target for Cancer Therapeutics. Clin. Cancer Res. 14 (16), 5000–5005. https://doi.org/10.1158/1078-0432.ccr-08-0746.

Mohammed, R.A.A., Ellis, I.O., Mahmmod, A.M., Hawkes, E.C., Green, A.R., Rakha, E.A., Martin, S.G., 2011. Lymphatic and blood vessels in basal and triple-negative breast cancers: characteristics and prognostic significance. Mod. Pathol. 24 (6), 774–785. https://doi.org/10.1038/modpathol.2011.4.

Morton, D.B., 2000. A systematic approach for establishing humane endpoints. ILAR J. 41 (2), 80–86. https://doi.org/10.1093/ilar.41.2.80.

Mukherjee, N., Bhattacharya, N., Alam, N., Roy, A., Roychoudhury, S., Panda, C.K., 2012. Subtype-specific alterations of the Wnt signaling pathway in breast cancer: Clinical and prognostic significance. Cancer Sci. 103 (2), 210–220. https://doi.org/10.1111/j.1349-7006.2011.02131.x.

Nakano, M., Fukami, T., Gotoh, S., Nakajima, M., 2017. A-to-I RNA Editing Up-regulates Human Dihydrofolate Reductase in Breast Cancer. J. Biol. Chem. 292 (12), 4873–4884. https://doi.org/10.1074/jbc.m117.775684.

Neophytou, C., Boutsikos, P., Papageorgis, P., 2018. Molecular Mechanisms and Emerging Therapeutic Targets of Triple-Negative Breast Cancer Metastasis. Front. Oncol. 8 https://doi.org/10.3389/fonc.2018.00031.

Newman, P.J., 1999. Switched at birth: a new family for PECAM-1. J. Clin. Invest. 103 (1), 5–9. https://doi.org/10.1172/jci5928.

Ota, H., Sakurai, M., Gupta, R., Valente, L., Wulff, B.-E., Ariyoshi, K., Iizasa, H., Davuluri, R., Nishikura, K., 2013. ADAR1 Forms a Complex with Dicer to Promote MicroRNA Processing and RNA-Induced Gene Silencing. Cell 153 (3), 575–589. https://doi.org/10.1016/j.cell.2013.03.024.

Patterson, J.B., Samuel, C.E., 1995. Expression and regulation by interferon of a double-stranded-RNA-specific adenosine deaminase from human cells: evidence for two forms of the deaminase. Mol. Cell. Biol. 15 (10), 5376–5388. https://doi.org/10.1128/mcb.15.10.5376.

Qin, Y.-R., Qiao, J.-J., Chan, T.H.M., Zhu, Y.-H., Li, F.-F., Liu, H., Fei, J., Li, Y., Guan, X.-Y., Chen, L., 2014. Adenosine-to-Inosine RNA Editing Mediated by ADARs in Esophageal Squamous Cell Carcinoma. Cancer Res. 74 (3), 840–851.

Robson, M., Im, S.-A., Senkus, E., Xu, B., Domchek, S.M., Masuda, N., Delaloge, S., Li, W., Tung, N., Armstrong, A., Wu, W., Goessl, C., Runswick, S., Conte, P., 2017. Olaparib for Metastatic Breast Cancer in Patients with a Germline BRCA Mutation. N. Engl. J. Med. 377 (6), 523–533.

Sagredo, E.A., Blanco, A., Sagredo, A.I., Pérez, P., Sepúlveda-Hermosilla, G., Morales, F., Müller, B., Verdugo, R., Marcelain, K., Harismendy, O., Armisén, R., 2018. ADAR1-mediated RNA-editing of 3′UTRs in breast cancer. Biol. Res. 51 (1) https://doi.org/10.1186/s40659-018-0185-4.

Sagredo, E.A., Sagredo, A.I., Blanco, A., Rojas De Santiago, P., Rivas, S., Assar, R., Pérez, P., Marcelain, K., Armisén, R., 2020. ADAR1 Transcriptome editing promotes breast cancer progression through the regulation of cell cycle and DNA damage response. Biochim. Biophys. Acta Mol. Cell Res. 1867 (8), 118716. https://doi.org/10.1016/j.bbamcr.2020.118716.

Saito-Diaz, K., Chen, T.W., Wang, X., Thorne, C.A., Wallace, H.A., Page-Mccaw, A., Lee, E., 2013. The way Wnt works: Components and mechanism. Growth Factors 31 (1), 1–31. https://doi.org/10.3109/08977194.2012.752737.

Sakurai, M., Shiromoto, Y., Ota, H., Song, C., Kossenkov, A.V., Wickramasinghe, J., Showe, L.C., Skordalakes, E., Tang, H.-Y., Speicher, D.W., Nishikura, K., 2017. ADAR1 controls apoptosis of stressed cells by inhibiting Staufen1-mediated mRNA decay. Nat. Struct. Mol. Biol. 24 (6), 534–543. https://doi.org/10.1038/nsmb.3403.

Sanhueza, C., Wehinger, S., Castillo Bennett, J., Valenzuela, M., Owen, G.I., Quest, A.F. G., 2015. The twisted survivin connection to angiogenesis. Mol. Cancer 14 (1). https://doi.org/10.1186/s12943-015-0467-1.

Sapino, A., Bongiovanni, M., Cassoni, P., Righi, L., Arisio, R., Deaglio, S., Malavasi, F., 2001. Expression of CD31 by cells of extensive ductal in situ and invasive carcinomas of the breast. J Pathol 194 (2), 254–261. https://doi.org/10.1002/1096-9896(200106)194:2<254::AID-PATH880>3.0.CO;2-2.

Schuh, J.C.L., 2004. Trials, Tribulations, and Trends in Tumor Modeling in Mice. Toxicol. Pathol. 32 (1_suppl), 53–66. https://doi.org/10.1080/01926230490424770.

Shah, S.P., Morin, R.D., Khattra, J., Prentice, L., Pugh, T., Burleigh, A., Delaney, A., Gelmon, K., Guliany, R., Senz, J., Steidl, C., Holt, R.A., Jones, S., Sun, M., Leung, G., Moore, R., Severson, T., Taylor, G.A., Teschendorff, A.E., Tse, K., Turashvili, G., Varhol, R., Warren, R.L., Watson, P., Zhao, Y., Caldas, C., Huntsman, D., Hirst, M., Marra, M.A., Aparicio, S., 2009. Mutational evolution in a lobular breast tumour profiled at single nucleotide resolution. Nature 461 (7265), 809–813. https://doi.org/10.1038/nature08489.

Shannon, P., Markiel, A., Ozier, O., Baliga, N.S., Wang, J.T., Ramage, D., Amin, N., Schwikowski, B., Ideker, T., 2003. Cytoscape: A Software Environment for Integrated Models of Biomolecular Interaction Networks. Genome Res. 13 (11), 2498–2504. https://doi.org/10.1101/gr.1239303.

Shin, S., Sung, B.-J., Cho, Y.-S., Kim, H.-J., Ha, N.-C., Hwang, J.-I., Chung, C.-W., Jung, Y.-K., Oh, B.-H., 2001. An anti-apoptotic protein human survivin is a direct inhibitor of caspase-3 and -7. Biochemistry 40 (4), 1117–1123. https://doi.org/10.1021/bi001603q.

Shtutman, M., Zhurinsky, J., Simcha, I., Albanese, C., D'Amico, M., Pestell, R., Ben-Ze'Ev, A., 1999. The cyclin D1 gene is a target of the -catenin/LEF-1 pathway. Proc. Natl. Acad. Sci. 96 (10), 5522–5527. https://doi.org/10.1073/pnas.96.10.5522.

Song, I.H., Kim, Y.-A., Heo, S.-H., Park, I.A., Lee, M., Bang, W.S., . . . Lee, H.J., 2017. ADAR1 expression is associated with tumour-infiltrating lymphocytes in triple-negative breast cancer. Tumor Biol., 39, 10, 101042831773481. https://doi.org/10.1177/1010428317734816.

Sun, B., Zhao, X., Ding, L., Meng, X., Song, S., Wu, S., 2016. Sunitinib as salvage treatment including potent anti-tumor activity in carcinomatous ulcers for patients with multidrug-resistant metastatic breast cancer. Oncotarget 7 (36), 57894–57902. https://doi.org/10.18632/oncotarget.11082.

Sung, H., Ferlay, J., Siegel, R.L., Laversanne, M., Soerjomataram, I., Jemal, A., Bray, F., 2021. Global cancer statistics 2020: GLOBOCAN estimates of incidence and mortality worldwide for 36 cancers in 185 countries. CA Cancer J. Clin. 71 (3), 209–249. https://doi.org/10.3322/caac.21660.

Sutherland, C., Leighton, I.A., Cohen, P., 1993. Inactivation of glycogen synthase kinase-3β by phosphorylation: new kinase connections in insulin and growth-factor signalling. Biochem. J 296 (1), 15–19. https://doi.org/10.1042/bj2960015.

United Kingdom Co-ordinating Committee on Cancer Research (UKCCCR) Guidelines for the Welfare of Animals in Experimental Neoplasia (Second Edition). (1998). British J. Cancer, 77(1), 1–10. https://doi.org/10.1038/bjc.1998.1.

Wang, Z., Li, B.o., Zhou, L., Yu, S., Su, Z., Song, J., Sun, Q.i., Sha, O.u., Wang, X., Jiang, W., Willert, K., Wei, L., Carson, D.A., Lu, D., 2016. Prodigiosin inhibits Wnt/β-catenin signaling and exerts anticancer activity in breast cancer cells. Proc. Natl. Acad. Sci. 113 (46), 13150–13155. https://doi.org/10.1073/pnas.1616336113.

Woodgett, J.R., 1990. Molecular cloning and expression of glycogen synthase kinase-3/factor A. EMBO J 9 (8), 2431–2438.

Wu, B., Crampton, S.P., Hughes, C.C., 2007. Wnt signaling induces matrix metalloproteinase expression and regulates T cell transmigration. Immunity 26 (2), 227–239. https://doi.org/10.1016/j.immuni.2006.12.007.

Xu, L.-D., Öhman, M., 2018. ADAR1 Editing and its Role in Cancer. Genes 10 (1), 12. https://doi.org/10.3390/genes10010012.

Yuan, Z.-Y., Luo, R.-Z., Peng, R.-J., Wang, S.-S., Xue, C., 2014. High infiltration of tumor-associated macrophages in triple-negative breast cancer is associated with a higher risk of distant metastasis. OncoTargets and Therapy 1475. https://doi.org/10.2147/ott.s61838.